T-PM-A1 THE DISTRIBUTION FUNCTION OF RATE CONSTANTS IN HYDROGEN EXCHANGE KINETICS. D.G. Knox and A. Rosenberg, Univ.of Minnesota, Minneapolis, MN 55455.

The exchange reactions of the amide protons located on the peptide backbone of proteins are a very powerful and general tool that may be used to probe the dynamics of protein functions. This technique has been extensively used to monitor a protein's response to changes in such variables as: temperature, pressure, pH, ionic strength, denaturants, substrate binding, protein-protein association and so on. However an analysis in terms of the individual sites does not immediately appear tractable.There are typically a hundred or more reactions that occur simultaneously. This great complexity, however, allows one to replace the following sum by an integral: $H_{rem}(t) = \sum e^{-k_i t} = \int_0^\infty f(k)\, e^{-kt}\, dk$. This equation defines a distribution function of rate constants by which the exchange proceeds. The f(k) can be calculated by taking the inverse Laplace transform of the exchange profile, Hrem(t). We have performed a series of matched experiments on lysozyme, and find at 25°C that: $f(k) = ba^{-n}\exp(-a(k-c))(k-c)^{n-1}/\Gamma(n)$ $k>c$. The exchange can be partioned into two parallel pathways for each site: solvent penetration of the native form and "thermal" unfolding. This decomposition may be substantiated by: its mathematical form, its free energy relative to the chemical exchange step, and the influences of trichloroethanol and glycerol. The temperature dependence of Hrem(t) yields the enthalpy distribution of exchange which is bimodal and sharp. The component of the distribution function due to solvent penetration (mobile defects) affords us some information concerning the spread and mean of the relaxation spectrum of the protein and on its response to even subtle perturbations.

T-PM-A2 A SOLUTION AND SOLID STATE STRUCTURAL COMPARISON BY ELECTRIC DICHROISM. Fritz S. Allen and Douglas R. C. Priore*, University of New Mexico, Albuquerque, NM, 87131.

We have developed a methodology to examine the structural consistency between solid state and solution preparations of macromolecules. We obtain polarized absorption spectra for an oriented solid state sample as well as solution electric dichroism data. If the molecular structure is the same in both samples the two sets of spectra must be related only by rotation. The angle of this rotation is given by the difference between the crystal or stretch axis in the solid state sample and the electrical axis which is oriented in the solution experiment. We presume the structures are identical and solve for this rotation angle. By comparing the resulting calculated rotational operator to a true rotational operator we can judge the validity of the initial postulate of structural consistency. We have applied this technique to oriented films and solutions of several nucleic acids. By decreasing the relative humidity of the oriented film when the polarized absorption spectra are taken, the rotation angle changes to reflect the B to A form transition in the solid state. The formalism and results will be described.

T-PM-A3 BREATHING MODES AND RESONANT MELTING OF THE DOUBLE HELIX. E.W. Prohofsky, K.C. Lu,* and B.F. Putnam*, Dept. of Phys., Purdue Univ., W. Laf., Ind. 47907.

Vibrational modes have been calculated for several duplex DNA polymers. Many modes appear which can be considered to be breathing modes in which the vibration involves separation of the two strands. Stimulation of these modes can cause large displacement between the strands which can enhance the probability of melting. The process requires less energy to bring about melting than heating as in the case of heating energy is thermally distributed among all the modes of the system rather than introduced resonantly into those most effective at bringing about melting. Crude estimates indicate that melting may be induced in aqueous environments over small regions for energy expenditures of the order of an electron volt. Energy can be transferred to these vibrational modes of the helix from vibrations in enzyme complexes if the complexes and helix are in physical contact. It is possible for enzyme systems in high vibrational states to enhance the melting of the helix if their vibrational frequencies are the same as the breathing modes of the helix. High vibrational states in enzymes can easily result from non-radiative damping of excited electron levels resulting from splitting energetic bonds such as those in the nucleoside triphosphates.

T-PM-A4 ROTATIONAL DIFFUSION AND FLUORESCENCE DEPOLARIZATION OF MACROMOLECULES WITH SEGMENTAL FLEXIBILITY. S.C. Harvey and H.C. Cheung, Biophysics Section, Department of Biomathematics, University of Alabama in Birmingham, Birmingham, AL 35294.

A method is given for the generation of fluorescence anisotropy decay curves for model macromolecules consisting of two rigid subunits connected by a hinge. To begin with, the elements of the resistance tensor must be determined either analytically or numerically, since the diffusion tensor depends both on these coefficients and on the bend angle restoring force[1]. In order to apply the Belford equation, the average rotational diffusion coefficients must be calculated in a way that takes into account the dependence of the resistance tensor on the particle shape, which changes stochastically. Specifically, the averaging procedure must include three considerations:

(1) The macroscopic manifestations of rotational diffusion correspond to rotations about the hydrodynamic center of reaction.
(2) As the molecule bends, a fluorophore rigidly attached to one subunit changes its orientation relative to the molecular coordinate system at the center of reaction.
(3) The bend angle probability distribution function for the ensemble of molecules is defined by the Boltzmann distribution of bend angle potential energies.

Anisotropy decay curves are given for model hinged rods, and the effects of hinge stiffness and hinge location are discussed. As an application of the method, model data are compared with experimental data from labeled myosin rods[2]. (Supported in part by USPHS Grant AM-14589 to H.C.C.)

1. S.C. Harvey (1978) J. Chem. Phys. 68, 3426.
2. S.C. Harvey and H.C. Cheung (1977) Biochemistry 16, 5181.

T-PM-A5 DIFFUSION CONTROLLED PROCESSES DESCRIBED BY THE SMOLUCHOWSKI EQUATION. Attila Szabo, Klaus Schulten*, and Zan Schulten*. Department of Chemistry Indiana University, Bloomington, IN 47401 and Max Planck Institute for Biophysical Chemistry, D-3400 Goettingen, West Germany.

There are a variety of problems (e.g. ligand binding to receptors, intrachain reactions of macromolecules) where one wishes to determine the average time (τ) required for a particle, diffusing under the influence of a potential, to reach and be bound by a target. The approach of Adam and Delbrück[1] is applicable only when the time-dependent diffusion equation is analytically soluble subject to appropriate boundary conditions. Even then the results are cumbersome. However, using the theory of first passage times, τ can be expressed in terms of an integral even when no analytical solution to the Smoluchowski equation exists. For problems involving free diffusion, this approach yields simple closed expressions. Finally, we show that a single exponential, using τ as the relaxation time, provides an excellent description of the entire time course of the reaction as determined by numerical solution of the appropriate differential equation. (Supported by NIH grant HL-21483).

[1]Adam, G. and Delbrück, M., in Structural Chemistry and Molecular Biology, p. 198 (Rich, A. and Davidson, N. eds., Freeman, San Francisco, 1968).

T-PM-A6 AN APPROACH FOR PREDICTING THE THREE-DIMENSIONAL STRUCTURE OF VARIABLE REGIONS OF IMMUNOGLOBULINS. J. M. Stanford* and T. T. Wu, Dept. of Biochemistry and Molecular Biology, Northwestern Univ., Evanston, Ill. 60201.

A procedure has been developed which generates possible three-dimensional conformations of variable regions of immunoglobulins. Since these proteins share the same three-dimensional structure except at their binding sites, the prediction of the conformation of an immunoglobulin's variable region reduces to the prediction of the conformation of the six hypervariable regions. An immunoglobulin whose atomic coordinates have been determined by x-ray diffraction analysis is used as a model for the framework; each hypervariable loop must then be of the proper length and orientation such that it can hook onto the framework. Several possible (ϕ,Ψ) angle choices for each residue in the hypervariable regions are made using the Wu-Kabat (ϕ,Ψ) angle selection procedure. An initial choice of the conformation of each hypervariable region is found by searching for the permutation of (ϕ,Ψ) angle pairs which produces a chain with roughly the desired length and amino and carboxyl terminal orientations. This initial choice is refined by allowing each individual angle to vary within $\pm$30 degrees. A fitting procedure based on a least squares fit then locates angle modifications which generate improved fits to the framework. As each hypervariable region's backbone conformation is predicted, steric hindrance is searched for and corrected. Finally, the hypervariable regions must combine with each other such that a binding pocket which can accomodate any known antigens is formed. The application of this technique to the immunoglobulin MOPC-315 has successfully produced a possible binding site structure. This work is supported by NIH-5-RO1-GM21482-04, NIH-NO1-RR-4-2147. TTW is an RCDA, NIH-5-KO1-AI70497-05.

T-PM-A7 TIME-DEPENDENT BIREFRINGENCE, LINEAR DICHROISM, AND OPTICAL ROTATION RESULTING FROM RIGID-BODY ROTATIONAL DIFFUSION. W. A. Wegener, R. M. Dowben, and V. J. Koester,* University of Texas Health Science Center, Dallas, TX 75235.

Expressions are derived for the time-dependent relaxation behavior of a monodisperse suspension of arbitrarily shaped rigid bodies, after initial alignment by an electric field in a Kerr cell. The analysis predicts that five exponential terms are required for a complete description of birefringence, linear dichroism, and optical rotation decay phenomena in a force-free rotational diffusion process. The overall relaxation expression can be partitioned into one factor called the distribution factor and another called the anisotropy factor. The distribution factor depends on the initial alignment conditions, as determined by the particular experimental technique employed. Consideration of this factor alone permits application to other alignments, e.g. by hydrodynamic flow or magnetic fields. The anisotropy factor involves the light scattering, absorption, or optical rotation properties of the body. Because of this partitioning, symmetry considerations can be applied independently to the anisotropy and distribution factors. Symmetry constraints that involve special relationships between tensor components of these factors and the diffusion tensor lead to a reduction in the number of required exponential terms. A particular symmetry led to the "two exponential" results of a previous treatment. Furthermore, we have obtained the explicit form for the coefficients of the exponential relaxation terms. Since these, as well as the rotational diffusion coefficients, can undergo changes with varying environmental conditions, they should be considered as important indicies of changes in macromolecular conformation. Our results demonstrate that the presence of three or more exponential terms in time-dependent birefringence measurements is not a sufficient criterion for determining macromolecular flexibility.

T-PM-A8 CAN ANY ARBITRARILY-SHAPED BODY BE REPRESENTED BY AN ELLIPSOID IN DIFFUSION SPACE? R. M. Dowben, W. A. Wegener, and V. J. Koester, University of Texas Health Science Center, Dallas, Texas 75235.

A general ellipsoidally-shaped body, or more commonly, an ellipsoid of revolution, serves as a convenient model for evaluating the rotational diffusion properties of macromolecules. If Perrin's equations for general ellipsoids can be shown to generate all possible rotational diffusion coefficients, then there would exist at least one equivalent general ellipsoidal shape for every arbitrarily-shaped rigid body. We evaluated the problem by first generating a space, r-space, representing all possible ellipsoidal shapes. We then generated another space, D-space, representing all possible combinations of rotational diffusion coefficients. We then mapped r-space onto D-space. Ellipsoidal shapes map onto diffusion space in a well-defined manner. The mapping is either 1:1, 2:1, or 3:1; several distinctly different regions of r-space map onto the same regions of D-space. Not all of D-space is covered by the mapping from r-space. Therefore, there are combinations of rotational diffusion coefficients that cannot be generated from ellipsoidally-shaped bodies. Examples of kinds of bodies that cannot be represented by an equivalent ellipsoidally-shaped body are bent rods, or two or more spheres connected by rigid arms. The three rotational diffusion coefficients generate five time constants. For ellipsoidally-shaped bodies, two pairs of time constants are almost degenerate. However, for diffusion coefficient sets that cannot be represented by a general ellipsoid, such degeneracy of the time constants may not occur. Therefore, the observation of more than three time constants in time-resolved experiments is not a sufficient criterion of macromolecular flexibility. (Supported by grants from the Sid W. Richardson Foundation and the NIH-HL-16678.)

T-PM-A9 GRIFFITH MODEL BONDING IN OXYGEN MANGANESE PORPHYRIN COMPLEXES.† L. K. Hanson,* and B. M. Hoffman* (Introduced by S. Feldberg), Brookhaven National Laboratory, Upton, NY 11973 and Department of Chemistry, Northwestern University, Evanston, IL 60201.

Manganoglobin, in which manganese porphyrins have been substituted for the heme prosthetic group, cooperatively and reversibly binds some small molecules but not oxygen. However, Mn(II) porphyrins do bind O_2 reversibly at -80°C in organic solvents to form pentacoordinated complexes in contrast to the hexacoordinated O_2 complexes formed by iron and cobalt porphyrins. The reaction with O_2 transforms the Mn(II) porphyrin spectrum from the normal to "hyper" type with a split Soret band typical of Mn(III) porphyrins. EPR spectra indicate a spin change from S = 5/2 to S = 3/2 and ^{17}O substitution indicates little unpaired spin density on the O_2. Analysis of the EPR data suggested that the O_2 molecule binds to the Mn in the Griffith mode (edge-on, parallel to the porphyrin plane) and that the complexes could be formally described as $Mn(IV)O_2^{=}$.[1] However, published ab initio calculations[2] predict instead that $Mn(III)O_2^{-}$ should be the most stable configuration, with O_2 bound in the Pauling mode (end-on, bent). Charge iterative extended Hückel calculations are reported here for both the Griffith and Pauling models for O_2·Mn porphins, in which the O-O, Mn-O, out of plane Mn distances and the O-O orientation above the porphinato plane have been varied. All of the experimental results can be explained in terms of the Griffith model but not the Pauling model. Furthermore, our calculations suggest that the ab initio results may simply be due to the use of too short an O-O distance. We conclude therefore that, unlike Co(II) and Fe(II) porphyrins, Mn(II) porphyrins bind oxygen in the Griffith mode in a manner similar to that found for Ti porphyrins.

[1] B.M. Hoffman, et al., JACS, 98, 5473 (1976). [2] A. Dedieu, et al., JACS, 99, 8050 (1977).

† This work was supported by the Division of Chemical Sciences, U.S. Department of Energy, Washington, D.C., under Contract No EY-76-C-02-0016.

T-PM-A10 THERMODYNAMIC COMPENSATION IN INTERACTING PROTEIN SYSTEMS. E.E. Saffen, Jr.* and P.W. Chun, University of Florida, Gainesville, Florida 32610.

Any interacting protein system will have a unique compensatory temperature, $\langle T_c \rangle$, at which the contributions of enthalpy and entropy to the association process are balanced. $\langle T_c \rangle$ may be evaluated from the expression

$$\Delta G^\circ_{(T)gross} = [\Delta G^\circ_{\langle T_s \rangle} + \langle T_c \rangle \Delta S^\circ_{(T)gross}] - T_{exp} \Delta S^\circ_{(T)gross}.$$

We have found in those associating systems we examined, specifically bovine liver L-glutamate dehydrogenase (GDH), glucagon, α-chymotrypsin at low pH and reduced carboxymethylated apoA-II from high density lipoprotein, as determined from a linear plot of $\Delta H^\circ_{(T)}$ versus $\Delta S^\circ_{(T)}$, that

$$\langle T_c \rangle = T_{exp} + \left[\frac{T_{exp} \Delta S^\circ_{(T)gross}}{\Delta C^\circ_{P(T)gross}}\right] \text{ as } T_{exp} \to T_s, \text{ the entropic temperature at which}$$

$\Delta S^\circ_{(T)} \to 0$. When the Van't Hoff and Gibbs-Duhem expressions are combined to determine the Hofmeister effect, it is possible to determine the compensatory temperature in a self-associating protein system perturbed by the presence of a Hofmeister series of anions. The principal determinants of the linear thermodynamic compensation process operating in any interacting protein system were found to be

$$\Delta S^\circ_{(T)gross} / \Delta C^\circ_{P(T)gross} = \langle \Delta T_c' \rangle / \langle T_{exp} \rangle, \text{ where } \langle \Delta T_c' \rangle = (\langle T_c \rangle - T_{exp}).$$

This work was supported by NSF Grant PCM 76-04367.

T-PM-A11 RESONANT INTERACTIONS BETWEEN BIOLOGICAL MOLECULES. L.L. Van Zandt*, (Intrc. by C. Beetz), Purdue University, W. Lafayette, IN 47907.

Forces between localized, oscillating vibrations on molecules show strongly resonant dependence on the relative frequencies of the two oscillators; i.e. there is a force between the vibrating parts of two molecules if the frequencies are the same but none if the frequencies are different. A vibrating site on a large molecule can attract another specific type of molecule out of a medium, one which has a vibrational mode at the same frequency, without influencing other types of molecules in the medium. These resonant forces are thus highly selective. Other pairs of molecules could similarly interact using vibrations at a different frequency. In a complex medium such as a cell, many different types of interactions could be assisted by these resonant forces without interfering with each other. These forces could be found to be useful in assisting some metabolic reactions. It is interesting that they are vulnerable to selective suppression or enhancement by externally applied electromagnetic radiation of correspondingly specific frequencies.

T-PM-A12 DYNAMICS OF SMALL AND LARGE AMPLITUDE MOTIONS IN POLYPEPTIDES AND OTHER MACROMOLECULES

R.M. Levy, and M. Karplus*, Harvard University, Cambridge, Mass. 02138

The small amplitude dynamics of a polypeptide α-helix has been studied by a vibrational normal mode analysis of the atomic motions about their equilibrium positions. Detailed information has been extracted concerning the magnitudes and correlations of thermal fluctuations in atomic positions. Fluctuations in the backbone helix dihedral angles ϕ and ψ, are $12^\circ - 15^\circ$. The fluctuations of adjacent dihedral angles are highly correlated and the correlation pattern is affected by the flexibility of the peptide dihedral angle. Time dependent autocorrelations in the motion of ϕ and ψ decay due to dephasing in less than 1 picosecond. Length fluctuations have been evaluated and exhibit a strong end effect; the elastic modulus of the helix has been calculated. Rigid and adiabatic total energy surfaces corresponding to dihedral angle rotations in the middle of the helix have been obtained and compared with the quadratic approximation to those surfaces. Of particular interest is the fact that hydrogen bonds play a relatively small role in the local dihedral angle fluctuations, though the hydrogen bonds are important in the energy of overall length changes. Dynamics of large amplitude atomic motions of hydrocarbon chains has been studied using a diffusive Langevin equation. Butane, heptane, and icosomane served as model compounds for the study of large changes in dihedral angles. Transitions between trans and gauche states occurred every 50 - 100 picoseconds in butane and less frequently in heptane and icosomane. Torsional motion appears to be concerted to some extent in heptane. Rate processes as well as equilibrium properties of these systems obtained using both gas phase and solvent modified intramolecular potentials are reported.

This work is supported by National Institute of Health.

T-PM-A13 CONFORMATIONAL ENERGY MINIMIZATION IN THE APPROXIMATION OF LIMITED RANGE INTERACTIONS. R.L. Jernigan, and S.C. Szu, Lab. of Theoret. Biol., NCI, NIH, Bethesda, MD 20014.

The most reliable theoretical method for determining the unique conformations of biological macromolecules is to exhaustively search conformational energy space. An inordinate number of degrees of freedom precludes the complete application of such a method to molecules of even moderate size. As an alternative, we have developed a simple general algorithm for minimizing approximate energies which include limited ranges of interactions. The requisite set of energies are those for regions of lengths 1 to k for all possible conformations; interatomic interactions are included only within the given regions. The algorithm proceeds stepwise from one end of the molecule to the other. At each step, the energy is minimized for the portion of the molecule from the terminus to successively distant units. Each such intermediate result is retained for later use in combination with non-overlapping regions. The final result is a combination of regions with the lowest total energy. This method has been applied to determine the minimum energies of several proteins; the regions considered were the possible regular secondary structure regions. Conformational energies were calculated by a method which is highly dependent on electrostatic energies. However, any method, including the empirical statistics of protein secondary structures, could be combined with the present algorithm. Conformations included were all possible α-helices with $k \leq 26$ amino acids, β-strands with $k \leq 13$, and a variety of shorter mixed conformations. Computation times for this case are very modest. Results compare favorably with the conformations as determined in X-ray experiments. The implication of this success is that the most significant interactions in a protein are often those within regular secondary structure segments.

T-PM-A14 ANISOTROPIC MOTION IN SATURATION TRANSFER ESR SPECTROSCOPY: APPLICATIONS TO BIOMOLECULAR SYSTEMS. M.E. Johnson, Univ. of Ill. Med. Center, Chicago, Ill. 60680 and Argonne National Laboratory, Argonne, Ill. 60439.

Anisotropic motional behavior is present in many biomolecular systems, thus the quantitative application of saturation transfer ESR (ST-ESR) spectroscopy to such systems requires a general understanding of the spectral effects of anisotropic motion in ST-ESR. As an empirical approach to this problem, we have studied the motional behavior in two well-defined phospholipid bilayer model systems: (1) dipalmitoylphosphatidylcholine (DPPC) with a fatty acid analog spin probe which exhibits nitroxide x-y axial averaging, and (2) DPPC with a cholesterol analog spin probe which exhibits nitroxide x-z axial averaging. At X-band (9.5 GHz) the ST-ESR behavior of the two systems is qualitatively similar, but differs somewhat in quantitative detail. At Q-band (35 GHz) the two types of motion are clearly distinguishable; in general, Q-band appears to be the frequency of choice for studying slow anisotropic motion (provided sample requirements can be met). These model systems have been used to analyze motional behavior during the aggregation of deoxy sickle hemoglobin (HbS). The extent of this aggregation is sensitive to the presence of phosphate allosteric effectors, increasing significantly upon adding 2,3-diphosphoglycerate (DPG) to "stripped" HbS, and upon substituting inositol hexaphosphate for DPG. Motional behavior during the late stages of polymerization is highly anisotropic, but the degree of motional anisotropy appears to be relatively independent of the extent of motional restriction produced by the aggregation process. Comparison with the lipid bilayer systems indicates that the HbS axis of rotational symmetry is approximately coincident with the magnetic z-axis of the tightly bound spin label. (Supported in part by the Research Corporation, the USNIH and the USDOE.)

T-PM-B1 RED CELL-MEMBRANE INTERACTIONS WITH SUB-MICROMOLAR CONCENTRATIONS OF INORGANIC MERCURY. H. C. Mel & T. A. Reed*, Donner Lab, Univ. of California, Berkeley, Calif. 94720

Actions of low concentrations of noxious agents such as mercury, of evident interest for environmental and human health studies, can also aid in elucidating mechanisms involved in normal cell-membrane function and regulatory processes. The technique of Resistive Pulse Spectroscopy (RPS) has proved valuable for investigating cell size, form, and cell-membrane deformability (Mel & Yee, Blood Cells, 1975). A more recent application, termed "dynamic osmotic hemolysis" has permitted fast kinetic investigations of membrane disruption induced by osmotic shock, and of subsequent cell-membrane recovery processes (Yee & Mel, Biorheology, 1978). Many RPS-measured properties have been found to be sensitive to low concentrations of chemical and biological agents. We present here some results for one such agent, $HgCl_2$, acting on normal RBC: (1) RBC ($\sim 10^5$/ml) exposed to 10^{-7}M $HgCl_2$ show an early-time shrinkage phase ($\sim$20 min), and a later time swelling (>45 min), compared with controls. Swelling is enhanced in medium of 200 mOsm as compared with 300 mOsm. (2) Cells "instantaneously exposed to $\geq 10^{-6}$M $HgCl_2$ display immediately-enhanced hemolysis (10-200 sec post exposure). For cells pre-incubated in the isotonic mercury medium this enhanced fragility is manifest down to 10^{-8}M, and the effect for 10^{-6}M is also increased. (3) An early time protection against hemolysis is observed for cells instantaneously exposed to concentrations of $\leq 10^{-8}$M. These types of effects depend upon the ratio of cell to mercury concentrations, consistent with the notion that the (Hg^{++})/surface area is a dominant factor. Some of these effects have been seen by previous workers (e.g. Weed, Eber & Rothstein, 1962; Lessler & Walters, 1973; Garrett & Garrett, 1974), but the speed and sensitivity of RPS measurements permit extending such studies into domains of shorter times and lower exposures, as well as to additional kinds of responses. (Supported by Biomed. & Environ. Res. Div. of D.O.E.)

T-PM-B2 ERYTHROCYTE ANION TRANSPORT AND PROTEOLYTIC DIGESTION OF BAND 3 PROTEIN M. L. Jennings* and H. Passow* (Intr. by J. H. Kaplan), Max-Planck-Institut für Biophysik, Frankfurt am Main, Germany.

A 95,000 dalton trans-membrane protein (band 3) is responsible for anion transport across the human erythrocyte membrane. Extracellular chymotrypsin cleaves at least 98% of the integral membrane protein in band 3 into two peptides, of apparent mw 60,000 (60K) and 35,000 (35K) daltons, with no inhibition of anion transport. The bifunctional inhibitor of anion transport, H_2DIDS (4,4'-diisothiocyano dihydrostilbene-2,2'-disulfonic acid), added to red cells after the chymotrypsin treatment, forms a covalent crosslink between the 60K and 35K peptides. One of the -N=C=S groups of the H_2DIDS reacts rapidly with the 60K peptide; the covalent attachment of the other -N=C=S group to the 35K peptide is slower, but may be driven to completion at pH 9.5 (1 hr,37°). Under the conditions used, all of the bound H_2DIDS is associated with inhibition of anion transport, and the extent of crosslinking of the 60K peptide to the 35K peptide is well over 90%. No other crosslinked products, e.g. 60K dimer, are detected. These results indicate that 1) each monomer of band 3 is one functional unit of anion transport, and 2) the 60K and 35K peptides may remain in the membrane as a native complex after the chymotrypsin treatment. Extracellular papain also cleaves the band 3 protein, but unlike chymotrypsin, strongly inhibits Cl-Cl exchange. The only detectable difference between the actions of these two enzymes on the band 3 protein is that papain removes about 5,000 daltons from the 35K chymotryptic peptide. The 60K peptides produced by chymotrypsin and by papain differ by at most six amino acid residues, and may be identical. The findings that the 35K chymotryptic peptide can react stoichiometrically with H_2DIDS, and is detectably altered by the inhibitory enzyme papain, constitute the first evidence that this peptide may have a role in the anion transport function of band 3.

T-PM-B3 FORCE RELAXATION AND PERMANENT DEFORMATION OF RED CELL MEMBRANE. E. Evans and D. Markle,* Duke University, Durham, North Carolina 27706.

Micropipet aspiration experiments on human red cells are used to investigate force relaxation and permanent deformation processes in the cell membrane. If surface extension ratios are less than 3 or 4:1, the red cell membrane can support constant shear forces for periods of time on the order of a few minutes with negligible increase in extension; when released, the red cell returns to its original, undeformed shape. When the membrane is kept extended for greater periods of time, permanent deformation is observed after the cell is released. The amount of residual deformation is proportional to the time period of extension and the level of membrane shear force. Thus, the character of the permanent deformation process is consistent with semi-solid behavior that is analogous to a Maxwell solid, i.e. the serial addition of elastic and viscous processes. Based on the observations, we formulate a constitutive relation for nonlinear surface deformations that serially couples the membrane hyperelastic component to a viscous process. In contrast to viscous dissipation as heat that occurs in rapid extension of a viscoelastic solid or in plastic flow of the material above yield, the viscous process in this case represents the rate of entropy production due to permanent molecular reorganization through relaxation of structural components. Data from red cell experiments give a value on the order of 10 surface poise for the coefficient of the viscous process; when normalized by the elastic shear modulus, this value provides a characteristic time limit to the domain of elastic solid behavior that is on the order of 10^3 seconds.

T-PM-B4 ELASTIC DEFORMATION OF RED CELL MEMBRANES. Y.F. Missirlis and M.C. Brain*, McMaster University, Hamilton, Ontario, Canada, L8S 4M1.

A new method of measuring the eleastic shear modulus of the red cell membrane is presented. It involves the aspiration of red cells into polycarbonate filters under positive hydrostatic pressure, fixing the deformed cells and measuring the single protrusion length as a function of pressure under SEM. It is shown that the stress-strain relationship for the membrane is linear in the range of elongations where the red cell does not become spheroid. Analysis of the data by the approximate method of Evans results in the mean shear elastic modulus of the membrane of normal human red cells to be 0.01 dyn/cm (N > 100). A quite similar value has been reported by several investigators by the use of the micropipette aspiration technique. However this new method is simpler, easier to work with, faster and above all it can provide information on many more cells from the same sample than the micropipette technique. This is especially useful when comparison of different populations of cells is important with regard to their mechanical properties (deformability). (Supported by the Muscular Dystrophy Association of Canada).

T-PM-B5 A RELATIONSHIP BETWEEN MEMBRANE LIPID FLUIDITY AND THE RATES OF OSMOTIC HEMOLYSIS OF HUMAN ERYTHROCYTES. K. Araki* and J. M. Rifkind* (Intr. by J. Froehlich), Gerontology Research Center, NIA, NIH, Baltimore City Hospitals, Baltimore, MD 21224.

We have previously reported that the rate of osmotic hemolysis can be altered by changing the cholesterol content of the erythrocyte membrane (Abstract, 31st Ann. Gerontological Soc. Meeting, Dallas, 1978) with an inverse relationship between cholesterol content and the rate of hemolysis. Since cholesterol is known to decrease mobility of the lipid matrix, these results suggested a possible relationship between the mobility of membrane components and the rate of hemolysis. In order to test this hypothesis we have looked at the effect on the rates of hemolysis of a number of different membrane modifications which alter the mobility of different components of the membrane. At the same time we have used spin labels in order to look directly at the effects of these modifications on the mobility of the membrane components and have used SDS polyacrilamide gel electrophoresis to test for crosslinking of membrane proteins. We have looked at the effect of reagents which dissolve into the membrane altering mobility without chemically reacting with any membrane components, e.g., Triton-X, ethanol, and chlorpromazine. We have also looked at the effect of Ca^{2+} (plus ionophore), which induces enzymatic crosslinking, as well as other reagents which directly crosslink proteins of the erythrocyte membrane, e.g., diamide and glutaraldehyde. As a result of these studies, we find that changes in the mobility of proteins which frequently go together with a decrease in deformability do not correlate with the rate of hemolysis. However, changes in lipid fluidity do correlate with the rate of hemolysis. Therefore, the rate of hemolysis seems to be determined by the stability of the membrane lipid matrix.

T-PM-B6 EFFECT OF ELEVATED IMMUNOGLOBULINS ON INTERCELLULAR ADHESION OF RED CELLS IN VITRO. Martin M. Lee and Peter B. Canham, Biophysics Dept., Univ. Western Ontario, London, Canada.*

Previous work indicated that erythrocytes in plasma will make contact on a coverslip, deform, and then slide together to form a two cell rouleau†. Factors influencing the process are cellular deformability and the rouleaux inducing agent (e.g. immune proteins). Blood samples were obtained from patients with multiple myeloma; the blood was analyzed for albumin and the immune proteins. We prepared dilute suspensions of cells in plasma. We used an inverted Nikon microscope with oil immersion optics and 16 mm camera. We focussed on two measurements, the adhesion length ratio, $L/(r_1+r_2)$, and the displacement, S, as a function of time, t (Fig. 1). Analysis of doublet formations in blood from three patients with elevated γ-globulin and normal albumin showed the following: (i) a linear relation between adhesion length ratio and time with a non-zero intercept (ii) an average sliding velocity $\Delta s/\Delta t$ of 0.34μm/s ± 0.08(SD) and (iii) a corr. coeff. of 0.97 between the rate of change of the adhesion length and the average sliding velocity. The importance of this finding is that transient analysis of the adhesion length ratio can be applied to non-sliding events (which occur for elevated fibrinogen) as well as the sliding events which occur in normal plasma or plasma with elevated immune protein.

FIG 1

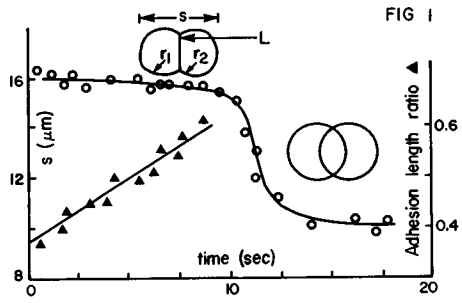

†Fung & Canham. Biorheology 11: 241, 1974.

*Supported by Ontario Heart Foundation.

T-PM-B7 DISTRIBUTION OF SUPEROXIDE DISMUTASE IN THE ERYTHROCYTE MEMBRANE. A. Petkau and T.P. Copps*, Medical Biophysics Branch, Whiteshell Nuclear Research Establishment, Atomic Energy of Canada Limited, Pinawa, Manitoba, Canada ROE 1LO and K. Kelly*, Immunology Department, University of Manitoba, Winnipeg.

Approximately 1% of the superoxide dismutase (SOD) in erythrocytes remains with their ghosts. On incubation with ^{125}I-labelled rabbit antibodies to bovine SOD, the uptake of the labelled antibodies by bovine erythrocytes and their ghosts is $1.2 \pm 0.4 \times 10^{-6}$ and $20 \pm 5 \times 10^{-6}$ cpm/cell, respectively. Higher uptake is observed with ghosts converted into inside-out vesicles, suggesting that the major portion of the membrane-associated SOD is located on the cytoplasmic side, consistent with its greater risk of oxidative attack from cellular sources of superoxide radicals. The existence of this asymmetric distribution is supported by enzyme assay data on normal intact ghosts and inside-out vesicles derived from them which, respectively, show 2.5 ± 0.6 and 10.5 ± 2.5 μg of SOD activity per mg protein.

The area density and distribution of the membrane-associated SOD are displayed by electron-microscopy of ghosts following reaction with ferritin-labelled antibodies. Transmission electronmicrographs (230,850X) of the outer surface of unfixed ghosts show an average ferritin particle density of $6.3 \pm 2.6/cm^2$. After glutaraldehyde fixation, this number is reduced to $1.4 \pm 0.5/cm^2$. This reduction, together with a shift in the frequency distribution of the particle densities, indicates that glutaraldehyde alters the distribution of SOD on the outer surface of red cell ghosts. The change may be the result of glutaraldehyde further internalizing the enzyme toward the cytoplasmic side where the particle density after fixation is $13 \pm 3/cm^2$.

T-PM-B8 10.5 A DIFFRACTION AND TRANSMEMBRANE PROTEINS OF THE ERYTHROCYTE GHOST. W. Lesslauer, Dept. of Pathology, Kantonsspital, CH-4056 Basel, Switzerland.

X-ray diffraction from oriented erythrocyte ghost membranes contains lamellar diffraction from the membrane stacking which defines the meridian, and equatorial bands centered at about 10.5 A. A meridional 1.5 A reflection is recorded after tilting the membranes by 31°. Side-to-side packed α-helices preferentially oriented normal to the membrane thus appear as structural element of the ghost. From biochemical data it is concluded that these α-helices belong to the glycophorin and band III proteins which probably are linked as dimers in intramembrane particles. The equatorial 10.5 A diffraction from sheep ghosts agglutinated by phytohemagglutinin appears stronger than in native ghosts even in specimens with similar mosaic spread. This may be due to higher order in agglutinated specimens or to α-helix content of the agglutinin, but small rearrangements of transmembrane proteins in the vicinity of the receptor sites must be considered also. Gross modifications such as intramembrane particle aggregation are excluded by SDS-polyacrylamide gel electrophoresis and freeze-etch electron microscopy. With agglutinated human ghosts a relatively sharp and disoriented 4.7 A band is recorded which is absent in parallel native ghost specimens. It can not be decided from the present data whether this band is due to a protein or a lipid component of the membrane, but it suggests that structural rearrangements can be induced in the membrane by the ligand binding at agglutinin receptor sites which may present a model for functionally relevant processes in other cell membranes.

T-PM-B9 X-RAY ANALYSIS OF CHLOROPLAST THYLAKOID MEMBRANE STRUCTURE. Jade Li* (Intr. by S. Lowey), Brandeis University, Waltham, Massachusetts 02154.

The structure of the chloroplast thylakoid membranes has been analyzed by X-ray diffraction. The stacked thylakoids of the grana lamellae were fractionated from shade plant chloroplasts and oriented by centrifugation and controlled dehydration. Lamellar diffraction patterns obtained at 25 Å resolution exhibit disorder effects indicating that the separation between different thylakoid membrane pairs is variable, and that within each membrane pair the pairing distance and the single membrane profiles are both variable. The diffraction data were analyzed using iterative procedures according to a strategy which treats the three aspects of disorder in separate stages. A self-consistent structural solution resulted which contained the average single membrane profile, the variation about this average in terms of the range of protein area fractions in the plane of the membrane, and the variations of the two membrane separations. The same average membrane profile was also obtained by analysis using the Monte Carlo approach. This average membrane profile shows an asymmetric bilayer with 34 Å between density peaks, and having higher electron density in the extra-thylakoid peak than in the lumen peak. It suggests that one fourth of the membrane area in the bilayer interior is occupied by proteins and pigment-protein complexes, and that these components protrude into the thylakoid lumen. These findings have been correlated with electron microscopic and biochemical observations.

(The advice and encouragement of Drs. R. Paul Levine and D.L.D. Caspar are gratefully acknowledged.)

T-PM-B10 SWELLING PROPERTY OF FROG SCIATIC NERVE. A. R. Worthington (*), C. R. Worthington and N. S. Murthy, Carnegie-Mellon University, Pittsburgh, PA 15213.

It has been noted previously that swelling of frog sciatic nerve takes place abruptly and different repeat distances are obtained in different experiments even when using the same immersion fluid. In a previous abstract (Murthy and Worthington, 1977) it was suggested that the swelling periods could be accounted for in terms of nw where n is an integer and w ≃ 5Å. In order to obtain a definitive answer to this question of discrete periods new swollen nerve patterns were recorded using a fixed specimen to film distances of 19 cms. Statistical analysis of the new x-ray data shows that the repeat periods do not follow this discrete behavior.

Certain swollen patterns of frog sciatic nerve show slanted lines. These patterns are inconsistent with discrete behavior and provide evidence that the repeat periods can change continuously along the length of the nerve fiber.

The swollen patterns of frog sciatic nerve are known to be reversible in that the normal pattern is regained on immersion in Ringer's solution. The live-to-swollen sequence is referred to as single swelling whereas the regained normal-to-swollen sequence is referred to as double swelling. Double and triple swelling patterns have been obtained. These patterns resemble the single swollen pattern but with generally increased repeat periods and slightly more disorder.

T-PM-B11 THE EFFECT OF HEAT ON FROG SCIATIC NERVE AS DETERMINED BY X-RAY DIFFRACTION. C. R. Worthington and A. R. Worthington (*), Carnegie-Mellon University, Pittsburgh, PA 15213.

Chemical treatments on nerve myelin are often carried out at elevated temperatures. It is therefore necessary to run control experiments in order to separately examine the effect of heat by itself. The effect of heat (increasing temperatures above room temperature) on sciatic nerve has been previously studied by Schmitt et al. (1941) and by Elkes and Finean (1953) using x-ray diffraction. Schmitt et al. (1941) reported that the 15-16Å equatorial spots in the wide-angle pattern persisted up to 70°C. Elkes and Finean (1953) noticed that at ≥ 58°C the normal low-angle x-ray pattern was replaced by two diffuse bands. We report that in the range of ≥ 58°C and ≤ 70°C the normal low-angle pattern disappears and is replaced by a new pattern of moderately sharp reflections. All reflections can be indexed as orders of d ≃ 435Å. By comparison with the low-angle x-ray patterns of acid-treated nerve myelin (Worthington, 1976) and with the swollen optic nerve patterns (Lalitha and Worthington, 1975) it is very likely that the heat-treated sciatic nerve is in the anolomous swollen state involving a repeat period of four membranes. X-ray analysis of the heat-treated x-ray pattern of frog sciatic nerve will be presented.

T-PM-B12 ISOLATION AND POLYPEPTIDE CHARACTERIZATION OF THE LUMINAL MEMBRANE OF MAMMALIAN URINARY BLADDER. J.A. Vergara (Intr. by H.C. Beall), Department of Anatomy, Duke University, Durham, North Carolina 27710.

The luminal membrane of mammalian urothelium shows a hexagonal structure with a unit cell side of 16 nm. The hexagons are close-packed on a p6 lattice and are made up of 6 subunits about 5 nm in diameter. Based on the low comparative density (1.14 g/ml) of this membrane, a method of isolation of this specialized cell surface, with minimal perturbation of the membrane matrix has been devised. Two major polypeptide bands 42,000 and 35,000 daltons are found by SDS polyacrylamide gel electrophoresis. Deoxycholate extracts all the bands except the 35,000 dalton polypeptide and this extraction preserves the hexagonal array of particles. Proteolytic digestion with trypsin, proteinase K and papain split the 35,000 dalton polypeptide to a 27,000 dalton polypeptide which remains attached to the membrane. No significant changes in the fine structure of the digested membranes have been observed so far at a resolution of 2 nm.

The significance of these results on the localization of the protein subunits in the lipid bilayer will be discussed.

Supported by NIH Grant #5-P01-GM23911.

T-PM-B13 RECONSTITUTED SARCOMPLASMIC Ca^{++} ATP-ase IS ELECTROGENIC. M. C. Goodall and Mark Habercom. Departments of Physiology and Biophysics, and Hematology, University of Alabama in Birmingham, Birmingham, Alabama 35294.

The question whether and under what conditions a given ion pump is electrogenic is of considerable theoretical importance. Using a modified Montal-Mueller technique (Goodall and Sachs, Biophys. J. 17:182a, 1977) we have reconstituted SR vesicles prepared according to Eletr and Inesi (BBA 282:174, 1972). (1) A bilayer reconstituted with phosphatidyl serine generates +30 to +40 mV opposite to the side on which ATP is added. (2) It is asymmetric, i.e., the catalytic site for ATP is on the monolayer formed from vesicles. (3) The K_m for ATP action is 10^{-5}-10^{-4}, i.e., about the same as in vitro ATP-ase. (4) This action is blocked by PCMBS (10^{-4} M) and La^{+++} (10^{-6} M). (5) The principal leak conductances are to Cl^-, H^+. (6) There is no evidence of K^+ conductance. (7) No potential develops if Cl^- is completely replaced by SO_4^{--}. (8) If HCl (~ 10^{-5} M) is added trans to ATP under these (i.e., all SO_4^{--}) conditions, oscillations of potential develop with a period of about 30 sec. (9) The equivalent short circuit current is 10^{-8} A cm^{-2}, i.e., about 10% of that carried by Ca^{++} in the intact vesicles. The possible role of counterion currents and their uncoupling by reconstitution will be discussed.

T-PM-B14 ACETYLCHOLINE RECEPTOR TOPOLOGY IN SEALED, ORIENTED MEMBRANE VESICLES. Paul R. Hartig and Michael A. Raftery, California Institute of Technology, Pasadena, California 91125

Osmotically intact membrane vesicles enriched in acetylcholine receptor have been isolated from Torpedo californica electric organ by density gradient methods. Alpha-bungarotoxin labeling studies reveal that approximately 95% of the intact acetylcholine receptor vesicles are obtained right-side out with their synaptic membrane faces exposed on the vesicle exteriors. Lactoperoxidase catalyzed iodination of these intact vesicles reveals membrane surface exposure of all four receptor subunits (40k, 50k, 60k, and 65k daltons) on the synaptic face. No evidence was obtained that any receptor subunit spans the membrane since acetylcholine receptor subunits did not label on the cytoplasmic membrane face. Carbamylcholine addition did not change the exposure of these receptor subunits. A 90k dalton polypeptide was labeled on both vesicle faces and thus spans the membrane.

T-PM-C1 A TRANSITION TEMPERATURE FOR THE MAXIMAL SODIUM CONDUCTANCE IN MAMMALIAN NODE OF RANVIER. S. Y. Chiu*, (Intr. by R. Tsien), Dept. of Pharmacol., Yale Univ., New Haven, CT 06510.

I have begun to examine the role played by membrane lipid in modulating function of excitable channels by looking for breaks in the electrical properties of the sodium channels in mammalian node of Ranvier when the temperature is varied. Voltage clamp studies, therefore, were carried out on single myelinated fibers from rabbit sciatic nerves over the temperature range 40°C-0°C. A single test depolarization to -20 mV preceded by a 100 msec hyperpolarizing prepulse to -125 mV to remove resting inactivation was used to assay sodium current every 0.4-0.6°C. The temperature dependence of $\bar{g}_{Na}$ was determined by extrapolating the decay phase of the sodium current back to the onset of the test depolarization. $\bar{g}_{Na}(T)$ determined this way shows a break at about 10°C. Thus, the Q_{10} for $\bar{g}_{Na}$, which is about 1.5 (in agreement with that reported for frog nerve) from 40°C to 10°C, becomes 3-5 below 10°C and the sodium current decreases markedly with decreasing temperature; the effect is reversible on rewarming. $\bar{g}_L$, in contrast, decreases smoothly with decreasing temperature from 40° to 0°C with a single Q_{10} of about 1.2. No distinct breaks were observed in the temperature dependence of τ_m and τ_h, the Q_{10} for both being about 3 between 25°-10°C and being slightly bigger than 3 below 10°C. E_{Na} measured at 37°C, 25°C, 15°C, and 0°C did not reveal a difference of more than ±5 mV. The break in $\bar{g}_{Na}(T)$ may be related to a phase change in the membrane lipid of the rabbit node.

Supported by grant NS-12327 from USPHS.

T-PM-C2 IS THE STEADY STATE INACTIVATION CURVE FOR THE SODIUM CHANNEL TEMPERATURE DEPENDENT? H. E. Mrose* and S. Y. Chiu* (Intr. by S.A. Lewis), Dept. of Pharmacol., Yale Univ., New Haven, CT 06510.

Voltage clamp experiments were performed on myelinated nerve fibers over the temperature range 24°C- 0°C. Hodgkin-Huxley analysis of sodium currents elicited by a single test step to -20 mV at intervals of 0.5°C showed that $\bar{g}_{Na}$, τ_h and τ_m vary smoothly with temperature over this range with Q_{10}'s of 1.3, 3 and 3, respectively; no discontinuity in the temperature dependence of these parameters was observed. Determination of the $h_\infty(E)$ and $P_{Na}(E)$ curves showed that both were shifted in a negative direction along the voltage axis when the temperature was lowered from 24°C to 0°C. However, the two curves were not shifted by the same extent; i.e., the negative shift in $h_\infty(E)$ exceeds that of $P_{Na}(E)$ by at least 10 mV. The $h_\infty(E)$ curve obtained at 0°C was less steep than that obtained at 24°C. The effect of temperature on the $h_\infty(E)$ was reversible on rewarming the fiber. The shape of the $P_{Na}(E)$ curve was not changed significantly by lowering the temperature. The values of E_{Na} measured at 24°C and 0°C did not differ by more that ±5 mV. The shift in the $h_\infty(E)$ curve with temperature suggests that the rate constants α_h and β_h have different Q_{10} values; this difference must be greater than that reported previously (Frankenheuser and Moore (1963), J. Physiol. 169, 431-437).

Supported by grant NS-12327 from USPHS.

T-PM-C3 EFFECTS OF HOLDING POTENTIAL ON GATING CHARGE MOVEMENTS. F. Bezanilla and R.E. Taylor, Dept. of Physiology, UCLA, Los Angeles, CA., NINCDS, NIH, Bethesda, Md. and MBL, Woods Hole, MA.

Non-linear charge movements, $Q(V) = \int_0^t I_g(z,V)dz$ (where I_g is gating current, V is membrane potential) were measured in internally perfused, voltage clamped squid axons. Potential steps were applied from a holding potential (HP) (which varied from -100 mV to +30 mV) to V. The P/4 averaging procedure was used with subtracting holding potentials (SHP) of -150 mV or +60 mV. The resulting Q(V) for t=2.5 msec, were fit to Q=Q0+QT/(1+exp((V0-V)/V1)). In any given axon, as the HP was made more positive, V0 became more negative, V1 increased and QT was virtually unchanged. (V0 = midpoint of the Q-V curve; (1/V1) is proportional to the valence times the distance between stable positions; QT = the total charge available to move.) For HP= -70 mV (5 expts) V0= -24±12 mV and V1=16±3.3 mV. For HP= -20 mV (5 expts) V0= -82±15 mV and V1=30±12 mV. Although the above expression for Q does not fit the data at HP= -70 as well as it does for more positive HP, it is clear from inspection of the data that in any given axon almost all of the effects of slow inactivation on Q(V) of depolarizing HP are the results of a simple shift along V by changes in V0. For an applied potential step to V= +10 mV immediately after restoration of HP from +20 to -70 mV Q(10) is about 1/2 normal which is entirely explained by the change in V0. With time, as V0 returns, Q(10) recovers with a time constant of about 30 seconds.

(We thank Drs. C.M. Armstrong and M. Cahalan for providing space and some equipment. Supported in part by USPHS Grant No. NS08951 and Biomedical Research program grant RRO 5354.)

T-PM-C4 DOES IMMOBILIZATION OF 'GATING' CHARGE REFLECT PROPERTIES OF Na INACTIVATION IN MYELINATED NERVE? W. Nonner* (Intr. by B. Hille), Univ. of Washington, Seattle, WA 98195.

Single, voltage clamped frog nerve fibers were stimulated with 'P/2' patterns for determining Na and 'gating' currents. 'Gating' current was corrected for slow components and leakage asymmetry, and integrated during the first 0.3 to 0.5 ms. The steady-state immobilization of 'gating' charge was examined after 45 ms conditioning pulses. Mobile charge was reduced over a similar range of prepotentials as the peak Na current. Charge immobilization, however, was incomplete leaving 1/3 of the charge after a prepulse to -18 mV, and it started at a less negative prepotential than Na inactivation. Development and removal of inactivation were studied by varying the length of the prepulse. Except for a small delay, Na current recovered in parallel to 'gating' charge. Near resting potential, however, Na current inactivated up to four times faster than 'gating' charge. For depolarizations $\geq$ -54 mV, the rates became similar, again. At -78 mV, Na current inactivated three times faster than it recovered. During a depolarization $\geq$ -46 mV, Na current decayed in two exponential phases. The reverse movement of 'gating' charge following the pulse was reduced as pulse length was increased, the rate reflecting the fast phase of Na inactivation. The similarities between Na inactivation and 'gating' charge immobilization suggest that both processes are linked. Na inactivation by itself appears to be part of a higher-order process that also affects charge mobility. During a depolarization (when Na channels are activated) the rate-limiting step seems to be the same for both processes, while different transitions become limiting at more negative potentials (when Na channels are not activated). This may indicate that activating 'gating' charges interact with an inactivation subunit.
Supported by Deutsche Forschungsgemeinschaft, SFB 38.

T-PM-C5 FAST KINETICS OF SODIUM CHANNEL GATING CURRENT. W.F. Gilly & C.M. Armstrong (Intr. by Clara F. Armstrong), Depts. Biology and Physiology, Univ. Pa., Philadelphia, Pa.

Experiments were performed on voltage clamped, internally perfused squid axons to characterize the kinetics of the earliest phase of gating charge movement (Ig) following a depolarizing voltage step. Ig during a small depolarization (ON Ig) is approximately exponential in time course; that for a large one has a distinct rising phase lasting for about 80 µs. The rise is not a machine artifact. Sampling time of the apparatus was 10µs/point, and a voltage step was complete within 30 µs. Tests show that the rising phase is not the result of nonlinear charge movement during the control pulses. 1) Over the range of -120 to -170 mV there is little nonlinear charge movement. Ig traces recorded with control pulses in this range nonetheless have a rising phase. 2) The rising phase is eliminated by a prepulse sufficient to inactivate gNa. This is true even for an asymmetrical pattern in which control pulses are not preceeded by a prepulse.

Ig following repolarization from a short step (OFF Ig) has a rising phase similar to that of ON Ig, but I Na recorded with the same pulse protocol has none, and falls approximately exponentially after the first 30-40 µs. 30mM external $ZnCl_2$ prolongs the rising phase of ON Ig but does not affect OFF Ig. These effects of Zn on Ig are consonant with those on I Na and show that the action of external Zn is not simply a modification of surface charge. We conclude that the rising phase of both ON and OFF Ig genuinely reflects properties of the gating process. The observations are compatible with a multistep model for gating in which some steps involve movement of a larger amount of charge than do others. They do not fit with the simple "m^3" scheme of gating.
Supported by NIH NS 12547.

T-PM-C6 TOXIN-RESISTANT SODIUM CHANNELS HAVE LOW CONDUCTANCE. F. Sigworth*, Department of Physiology, Yale University, and B. Spalding, Departments of Physiology, University of Washington and University of Rochester.

Carboxyl-modifying reagents have been shown to render Na channels resistant to block by TTX and STX (e.g. Baker and Rubinson, Nature 257, p.412, 1975; Spalding, Biophys. J. 21, p. 41a). We now find that trimethyloxonium ion (TMO)-modified, toxin-resistant channels in frog node of Ranvier have a lower (2.3 pS) conductance than normal (7 pS). Their single-channel current-voltage relationship shows less rectification and is similar to that of normal channels in reduced (20 mM) external Na. We suspect that the change in i-V behavior is due to the removal of a negative charge at the toxin receptor, changing the local potential and cation concentration.

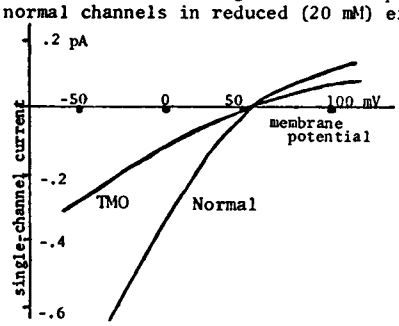

The figure shows the measured instantaneous I_{Na}-V relationships, scaled to match single-channel current estimates from ensemble fluctuation experiments (Sigworth, Nature 270, p.265). We observe a reduction in Na current after TMO treatment that is entirely accounted for by the change in conductance of some of the channels; hence TMO does not seem to destroy channels. The modified channels show no significant change in voltage-dependence or kinetics of gating.
Supported by USPHS grants NS12962, NS08174, GM07270.

T-PM-C7 STUDIES OF ION COMPETITION BETWEEN Na^+ and K^+ IONS IN THE PATHWAY OF EARLY CONDUCTANCE (i.e. "Na^+ CHANNEL") IN SQUID GIANT AXON. D.C. Chang, Dept. of Physics, Rice Univ. and Depts. of Physiol. and Pediatrics, Baylor College of Med., Houston, TX 77030.

The ion competition between Na^+ and K^+ in the pathway of early conductance (i.e., "Na^+ channel") was studied by examining the magnitude of the early current (under voltage-clamp conditions) as a function of concentration gradients of sodium and potassium ions. Using a double perfusion technique, the concentrations of Na^+ and K^+ were controlled both at the inside and at the outside of the axon. For simplicity of interpretation, we chose to study the outward current under conditions where the artificial sea water contains no Na^+ ions (Na^+ is being replaced by choline ion). Three techniques were used to separate the early outward current from the delayed outward current: (1) We used a 20 millisecond prepulse (of 60 mv hyperpolarization) to enhance the magnitude of the early current. (2) 20 mM of tetraethylamonium (TEA) was applied inside of the axon so that the delayed current was suppressed. (3) We used Cs^+ ions to replace some of the K^+ ions so that the delayed current was reduced. The preliminary results indicate that the Na^+ - K^+ competition is not of a linear fashion and the observed results are sensitive to the method of ion substitution. (Supported by USPHS grant GM-20154 and ONR contract N00014-77-C0092)

T-PM-C8 INTERFERENCE WITH SODIUM INACTIVATION GATING IN SQUID AXONS BY INTERNAL MONOVALENT CATIONS. G.S. Oxford and J.Z. Yeh, Dept. of Physiology, Univ. of North Carolina, Chapel Hill, NC 27514 and Dept. of Pharmacology, Northwestern Univ. Med. Schl., Chicago, IL 60611.

Normal sodium channel inactivation in internally perfused squid axons is incomplete. A second open state of the channel has been suggested to account for this observation (Chandler & Meves, 1970; Bezanilla & Armstrong, 1978). We examined this phenomenon in voltage-clamped squid axons in which internal K^+ was substituted by either Cs^+, TMA^+, $Tris^+$ or Na^+. In the presence of internal Cs^+ the ratio of residual Na current at the end of long depolarizing pulses (I_f) to peak Na current (I_p) at +80 mv averaged 0.13. Comparable residual currents were observed in normal internal $^pK^+$ by a TTX-subtraction technique. TMA^+ substitution for Cs^+ reduced I_p, but increased I_f, thus greatly increasing I_f/I_p (0.31 at +80 mv) and resulting in crossing of current traces in the two solutions. Tris substitution also increased I_f/I_p, but greatly suppressed both I_f and I_p. These results were obtained both in the presence of internal F^- and in F-free glutamate solutions. Changes in the ratio of I_f/I_p are manifested as changes in the 'foot' of the steady-state inactivation-voltage (h_∞) curve determined by double pulse methods. For example, the value of h_∞ at +80 mv in Cs^+ averaged 0.15, comparable to the I_f/I_p ratio, however, TMA^+ increased h_∞ to 0.45, greater than the corresponding I_f/I_p ratio. Experiments were performed in varying internal and external Na^+ concentrations in order to compare channel gating during inward Na current to that during outward Na current at the same voltages. I_f/I_p values were greater for outward current than for inward current from -30 to +80 mv. These observations are consistent with a model in which TMA^+, Na^+, and perhaps Cs^+ and K^+ interfere with the inactivation process by competing with a channel gating component for a site near the internal channel surface.
Supported by NSF grant BNS 77-14702 and NIH grants R01 GM-24866 and K04 GM-442.

T-PM-C9 EVIDENCE THAT THE K CHANNEL OF SQUID AXONS IS A MULTIPLE ION PORE. T. Begenisich and P. De Weer, Department of Physiology, University of Rochester, and Department of Physiology, Washington University.

Potassium ion fluxes through the K channel of squid giant axons cannot be described by the Üssing flux ratio equation for independent ion movement unless the right hand side is raised to a power n:

$$m_e/m_i = \exp(V_m - V_k)n/RT$$

Since V_m and V_x can readily be determined, all that is needed to compute n is the efflux, m_e, and influx, m_i. These fluxes were obtained by 3 methods: (1) K^{42} influx and total current, I_k, were measured and efflux was calculated ($m_e = I_k + m_i$); (2) K^{42} efflux and I_k were measured and influx was computed; (3) both K^{42} influx and efflux were directly measured. At $V_m = V_k$ the potassium conductance, g_k, is given by $g = nF^2m_i/RT$. We, therefore, measured g_k and m_i and calculated n. All four techniques gave similar n values which ranged from about 1.6 (V_m = -8mV, K_i = 200 mM) to about 3.2 (V_m = -38 mV, K_i = 350 mM). Depolarizing V_m and lowering internal K reduces n. These results suggest that a potassium pore may be simultaneously occupied by as many as 3 K ions.

T-PM-C10 K^+ CONDUCTION PHENOMENA APPLICABLE TO THE LOW FREQUENCY IMPEDANCE OF SQUID AXON. Harvey M. Fishman and Ronald D. Grisell*, Department of Physiology and Biophysics, University of Texas Medical Branch, Galveston, Texas 77550.

The observation of peaking in power spectra of K^+ current noise in squid axon (Fishman, Moore and Poussart, 1975, J. Memb. Biol. 24: 305) implies a kinetic scheme that is not described by a single, first order rate process. To confirm the noise data a low frequency K^+ conduction feature was calculated and measured in the linearized impedance/admittance function (Fishman, Poussart, Moore and Siebenga, 1977, J. Memb. Biol. 32: 255). However, it is important for kinetic models to distinguish between (1) the overall K conduction process in an axon, which includes phenomena arising from structures surrounding the axon, and (2) phenomena that occur exclusively in the excitable membrane. We have considered two physical phenomena, one within and the other outside of the excitable membrane, that might account for the low frequency impedance feature. The linearized HH equations are modified to take into account the accumulation of K^+ in a space outside the axon in conjunction with diffusion through the Schwann cell layer. The accumulation-diffusion model yields an admittance that has a low frequency mode that is similar in some respects to that observed experimentally. Alternatively, a hypothetical K^+ inactivation process, with a voltage-dependent time constant, gives a better account of the data. Either or both of these phenomena could be involved in producing the low frequency impedance behavior in the squid axon. Supported by NS-11764 and NS-13778.

T-PM-C11 THE COLE-MOORE DELAY: COOPERATIVITY AMONG POTASSIUM CHANNELS? F. Sigworth*, Department of Physiology, Yale University, New Haven CT 06510 (intr. by C. Stevens).

Long-range interactions between channels could (Changeux et al, PNAS 57, p.335, 1966) give rise to the high-order kinetics observed in the delayed activation of potassium conductance after a hyperpolarization (Cole and Moore, Biophys. J. 1, p.1, 1960). However, I find no evidence for such cooperativity from the results of an ensemble fluctuation experiment. A frog node of Ranvier was voltage clamped at 5° in TTX, and the mean and variance were computed point-by-point from ensembles of 400 current records evoked by identical pulse patterns (Sigworth, Nature 270, p.265, 1977). The figure shows the time course of the mean current and variance from depolarizations to 60 mV, preceded by -120 mV, 50 ms prepulses. The theoretical variance curve, calculated from the mean using binomial statistics, is based on the assumption of independent channels having one nonzero conductance level. It uses the same single-channel current value (0.6 pA) as the fit to the variance obtained without a prepulse. Cooperativity, appearing as correlations in the opening of channels, would result in larger variance values than predicted by the theory. This result is therefore consistent with the strict independence of gating in potassium channels, with the hyperpolarization delay arising from a process occurring in each channel.

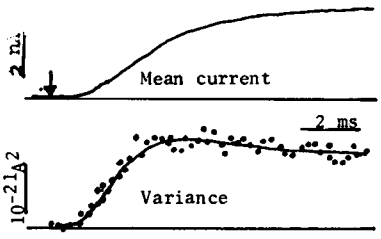

Supported by USPHS grant NS08174.

T-PM-C12 ELECTROLYTE PERMEABILITY OF NERVE MEMBRANES. D. Landowne and V. Scruggs, Department of Physiology and Biophysics, University of Miami, Miami, Fla. 33101.

Electrical nerve impulses are generated by a current of sodium ions passing through the nerve cell membrane. We have found that the current-voltage-concentration relationship is the simple sum of Fick's Law and Ohm's Law. That is

$$I = -P(c_o - c_i)F + (ac_o + bc_i)FV$$

where P is the permeability; c_o and c_i, the concentrations of ions on the two sides; F, Faraday's constant; a and b, the membrane acceptance (or specific conductance) of ions from the two sides; and V, the electrical potential. For sodium ions through squid axon membranes P is about 10^{-4} cm/sec; a, 10^{-6} and b, 3×10^{-6} cm/mV-sec. $P/(a+b) = 25 \pm 1$ mV (6) or kT/e. Thus only two constants are required to describe the membrane, either a and b or P and b/a where b/a is a measure of the membrane asymmetry towards sodium ions. An equivalent circuit with values for the potentials and conductances is shown to the side.

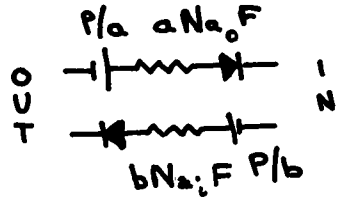

T-PM-C13 THERMODYNAMICALLY BASED CONTINUUM DIFFUSION THEORY COMPATIBLE WITH MODERN MEMBRANE DATA. T. L. Schwartz, University of Connecticut, Storrs, Ct. 06268.

A new physically rigorous formulation of membrane diffusion theory, based on thermodynamics has been used to demonstrate that inaccuracies in both the constant-field theory and the "independence principle" are due to overly approximate physical assumptions and not to a failure of continuum theory. This new theory is now shown to be specifically applicable to thin membranes as well as to thick ones. Its ability to determine the sum of the phase-boundary potentials from simple I-V data is shown to be general and not limited to the case of monotonic piecewise-continuous intramembrane electric fields as was implied by its earlier derivation. It is also demonstrated to solve several problems previously thought to be beyond the scope of continuum theory. Thus it shows that permeability, rigorously defined, is generally expected to vary with both voltage and concentration. This removes the previously puzzling difference between permeabilities measured from reversal potential shifts as compared to those measured from current ratios. The theory predicts that the ratio of permeabilities of a pair of ions simultaneously permeating a single channel type will probably be concentration dependent due to blocking and other effects, but will not be voltage dependent. Such ratios had been observed, but could not be explained by the constant-field continuum approach. This feature of the new theory also provides a basis for understanding "mole-fraction" effects. The measureability of the phase-boundary potential sum provided by this new approach suggests that effects due to mobility changes can now be separated from those due to partition coefficient changes. This possibility arises from the fact that the partition coefficient no longer appears only in product with the mobility, as it did in the constant-field theory where asymmetric boundary effects were rather arbitrarily defined away.

Supported by the University of Connecticut Research Foundation.

T-PM-D1 RELATION BETWEEN INTRACELLULAR Na ION ACTIVITY AND POSITIVE INOTROPIC ACTION OF SHEEP CARDIAC PURKINJE FIBERS. C.O. Lee, D.H. Kang*, J.H. Sokol*, and K.S. Lee*, Dept. of Physiology, Cornell Univ. Med. Coll., N.Y., N.Y. 10021.

Intracellular Na ion activity (a^i_{Na}) and tension (T) of the fibers were measured with Na^+-selective glass microelectrodes and a mechano-electric transducer before, during and after exposure to a cardiac glycoside, dihydroouabain (DO) of 5 x 10^{-8}, 10^{-7}, 5 x 10^{-7}, 10^{-6}, and 5 x 10^{-6} M. The exposure time was 15 min. for each dose. Before the exposure, the fibers were stimulated for about 20 min. to measure the normal tension (T_c). The stimulus rate was 60/min. throughout this experiment. The results are summarized in the table:

		Concentration (M) of DO			
	normal	10^{-7}	5 x 10^{-7}	10^{-6}	5 x 10^{-6}
	(n=11)	(n=4)	(n=8)	(n=5)	(n=3)
a^i_{Na}(mM)	6.4 ± 2.3	8.4 ± 2.5	14.1 ± 3.2	18.0 ± 4.0	29.6 ± 4.5
T/T_c	1	1.4 ± 0.4	2.7 ± 0.5	4.7 ± 1.0	8.0 ± 1.6

In the fibers exposed to 5 x 10^{-8} M DO, no changes in a^i_{Na} and T were observed. The results show that the relationship between the increase in a^i_{Na} and T/T_c is linear. It was also observed that the time course of the increase in a^i_{Na} was similar to that of the increase in T. In those fibers which recovered, the time courses of recovery of a^i_{Na} and T were similar. The results in this study strongly suggest that the positive inotropic action in the fibers is related to the increase of intracellular Na ion activity. (Supported by USPHS HL 21136 and HL 21014).

T-PM-D2 RESTING MEMBRANE AND POTASSIUM EQUILIBRIUM POTENTIALS IN SHEEP PURKINJE FIBERS. S-S Sheu*, M. Korth*, and D.A. Lathrop* (Intr. by H.A. Fozzard), Univ. of Chicago, Chicago, Il. 60637.

Intracellular K^+ activity (a^i_k) was continuously measured with K^+-sensitive liquid ion-exchanger microelectrodes during extracellular K^+ concentration ($[K^+]_o$) changes. In normal sodium containing (150mM) and sodium poor (2.5mM) Tyrode solutions, membrane resting potential (E_m) followed the calculated potassium equilibrium potential (E_k) at $[K^+]_o$ 12 to 100mM. A progressive separation of E_m from E_k occurred at lower $[K^+]_o$, though a^i_k remained constant and E_k showed the predicted Nernstian slope. The deviation of E_m from E_k was largest at $[K^+]_o$ lower than 2.7mM with normal sodium where a low level of E_m (~-30mV) is established and $E_k - E_m$ ~-120mV at 0.5mM$[K^+]_o$. The reduction of $[Na^+]_o$ to 2.5mM produced hyperpolarization of E_m and thus shifted E_m closer to E_k, but a difference of 20 to 30mV was still apparent at 0.5mM$[K^+]_o$. In conclusion, the deviation of E_m from E_k probably reflects a change in membrane permeabilities and not in a^i_k.

T-PM-D3 SODIUM CURRENTS IN RABBIT CARDIAC PURKINJE FIBERS. T.J.Colatsky and R.W.Tsien, Department of Physiology, Yale University School of Medicine, New Haven, Connecticut 06510.

Previous studies of cardiac sodium currents under voltage clamp have been criticized because of doubts about the adequacy of voltage control. Voltage nonuniformities are expected from the complex structure of heart muscle. Using the rabbit Purkinje fiber, a cardiac preparation with simple morphology, we have been able to record with the two-microelectrode voltage clamp method excitatory sodium currents (I_{Na}) meeting several criteria for satisfactory voltage control. Resolution and control of I_{Na} was improved by using short (450-700 μ) preparations, lowering external sodium and cooling to 13-23°C. Under these conditions, the activation of I_{Na} can be largely separated from the decay of the capacity transient. Adequate voltage control is suggested by the following observations: (1) inward current records show a smooth decay, with no secondary humps or notches; (2) the time course of the current is unchanged when its magnitude is varied by prepulse inactivation; (3) the measured reversal potential lies close to the expected value; (4) activation is a gradual function of membrane potential; and (5) tail currents following repolarization at peak I_{Na} decay smoothly and rapidly. These experiments indicate the feasibility of characterizing the sodium channel in intact mammalian cardiac muscle, and open the way for the direct analysis of its pharmacologic properties.

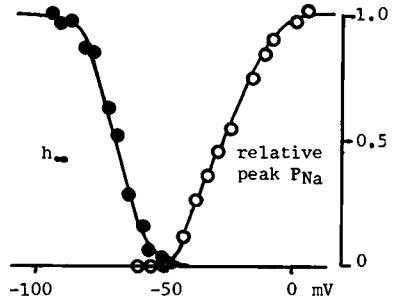

T-PM-D4 PACEMAKER PROPERTIES OF VOLTAGE-CLAMPED EMBRYONIC HEART CELLS. R. D. Nathan, Department of Physiology, Texas Tech University School of Medicine, Lubbock, TX 79430.

Spheroidal aggregates of 7-day embryonic chick heart cells were subjected to microelectrode voltage clamp. In 1.8 mM potassium, net "steady state" current was minimized at a holding potential of about -50 mV, which corresponds to the resting level in TTX. At more positive potentials, current was outward going and either increased (V < -33 mV) or decreased (-40 mV < V < -50 mV) with time. At potentials negative to -50 mV, net current increased with time in the inward direction. TTX reduced inward current at a holding potential of -62 mV consistent with its effects on pacemaker activity--a decline in the slope of the pacemaker potential and in the rate of beating just previous to action potential blockade. Clamping the potential to -40 mV during the early phase of diastolic depolarization resulted in outward going current which declined toward zero. Following a 0.5-sec prepulse to activate outward current, outward current tails were recorded (in TTX) during test pulses between -114 mV and -40 mV. Reversal potentials for these tails were -114 mV, -70 mV and -50 mV when measured in external potassium concentrations of 2.1 mM, 12 mM and 21 mM, respectively. The approximate 60-mV shift of E_R for a 10-fold change in $[K^+]$ suggests that this current is carried by potassium ions. If the clamp was turned off during the outward current tail, the membrane potential hyperpolarized followed by a slow diastolic depolarization. Hyperpolarization was enhanced (and pacemaker slope reduced) by removing the clamp during the early phase of the tail. When this procedure was repeated during the flow of inward current, the potential depolarized rapidly, initiating an action potential. These results are similar to those obtained by Noma and Irisawa in rabbit sinoatrial node cells (A. Noma and H. Irisawa, Pflüg. Arch. 366: 251, 1976). Supported by NIH grant HL 20708.

T-PM-D5 A KINETIC MODEL FOR DETERMINING THE CONSEQUENCES OF ELECTROGENIC ACTIVE TRANSPORT IN CARDIAC MUSCLE. J.M. Kootsey, Andrews University, Berrien Springs, MI; J.B. Chapman, Monash University, Victoria, Australia; E.A. Johnson*, Duke University Medical Center, Durham, NC.

In a continuously active tissue, such as cardiac muscle, electrogenic active transport constrains the passive membrane currents and both are significant in the generation of the action potential. A kinetic model of electrogenic active transport of sodium and potassium ions has been developed based on thermodynamic considerations and published experimental data. The model includes explicit dependence of sodium and potassium pump currents on transmembrane potential and on ion concentrations on both sides of the membrane. This model of active transport has been coupled to a system of passive permeabilities, of minimum degree of complexity, to simulate the integrated activity of active and passive ion transport in the generation of the cardiac action potential. Differential equations were integrated for the ion concentrations as well as for the membrane potential so that the pump current varied throughout the electrical cycle and with the rate and pattern of stimulation. The results of preliminary simulations indicate that electrogenic active transport provides a mechanism for slowly changing currents within the time scale of an action potential and also over a period of many action potentials. Electrogenic active transport thus complicates the separation of currents in the analysis of membrane properties. Unidirectional fluxes of ions have also been computed in the simulations and these too are altered by the presence of electrogenic active transport. Supported by a grant from NIH (2-P01-HL 12157).

T-PM-D6 PACEMAKER CURRENTS AND EXTRACELLULAR K^+ ACTIVITY IN RABBIT SA NODE. J. Maylie*, J. Weiss*, and M. Morad. Department of Physiology, University of Pennsylvania, Philadelphia, PA 19104.

The pacemaker potential in spontaneously beating SA nodal strips (diameter 0.3-0.5 mm) was studied using a single sucrose gap voltage clamp technique (Goldman & Morad, J. Physiol. 268:613, 1977). A time dependent, inward current (Ip) was recorded when the pacemaker potential was clamped at maximum diastolic potential (MDP). Hyperpolarizing clamps below MDP (up to -160 mV tested) increased the activation of Ip and failed to reverse it. The failure to reverse Ip was consistently observed in solution containing 2.7, 5.4, 8.1 mM KCl. The membrane conductance in response to small clamp perturbation (±10 mV) about the diastolic potential was constant (within 5%). K^+ activity in the paracellular space was measured with a double-barrelled K^+-selective μ-electrode. K^+ accumulation of 0.01 to 0.1 mM were recorded per single beat. Holding the membrane potential at MDP resulted in a linear depletion of K^+ during the development of Ip, suggesting no marked change in K^+ fluxes. At more positive or negative potentials to the pacemaker range, the rate of accumulation or depletion of K^+ increases with time. The lack of a reversal potential for Ip around E_K, and little or no membrane conductance change, seems to suggest that the pacemaker potential is generated primarily by an ionic species with a large positive equilibrium potential. Larger decreases in g_K would be required to generate the pacemaker potential than those indicated by K electrode or membrane conductance measurements. (HL 16152).

T-PM-D7 MEMBRANE PROPERTIES OF RAT SKELETAL MUSCLE IN PRIMARY TISSUE CULTURE.
M. Merickel, and R. Gray*, Baylor Col. of Med., Houston, TX. 77030.

We have studied embryonic rat muscle in primary tissue culture after myotube formation. The resting potential increased to an average value of -60 mV after 10 days in culture. These fibers had an input resistance of 1-2 MegOhms and exhibited pronounced delayed rectification. The action potential (a.p.) was well developed with the following average characteristics: 1) Amplitude, 80 mV; 2) Half amplitude duration, 9ms; and 3) After hyperpolarization of 15 mV and > 1 sec time course. The a.p. was typically sensitive to TTX at 10^{-6} M concentrations. TTX application substantially reduced the amplitude and rate of rise and also prolonged the duration of the a.p., uncovering a Ca^{++} component of the a.p. Prolonged application of TTX usually made the fiber completely electrically inexcitable which was reversible after return to normal Ringers solution. The contribution of Ca^{++} to the a.p. was examined by the use of Ca^{++} inhibitors (eg. Co^{++}) and substitutes (eg. Ba^{++}). Equimolar substitution of Ba^{++} for Ca^{++} produced a distinct shoulder on the falling phase of the action potential, while Co^{++} substitution significantly reduced the amplitude and prolonged the duration of the a.p., indicating the importance of Ca^{++} in the a.p. These substitutions for Ca^{++} also significantly reduced the amplitude and especially the duration of the after-hyperpolarization which suggests that the long duration of the after-hyperpolarization is due to a Ca-activated K-current. Ba^{++} and Mn^{++} substitution for Ca^{++} caused an input resistance increase, membrane potential oscillations and repetitive firing.

T-PM-D8 CHARGE MOVEMENT AND MECHANICAL ACTIVATION IN STRETCHED MUSCLE FIBERS.
C.S. Hui* and W.F. Gilly, Physiology Dept., Yale Univ. Medical School, New Haven CT.

We have performed measurements of charge movement using the 3-electrode voltage clamp technique at the end of frog twitch fibers. Depending on sarcomere length to be studied, whole muscles, small bundles of fibers, or isolated single fibers were bathed at about 7° C in an isotonic Ringer containing 115mM TEA-Cl, 11.8mM $CaCl_2$, 5mM RbCl, 2mM tetracaine and TTX. Nonlinear charge movement over the voltage range of -80 to +20 mV was observed in every fiber studied at sarcomere lengths up to 3.8μ. Total movable charge, Q_{max} (in nC/μF), did not appreciably diminish with fiber stretch, and results are summarized below (± 1 SEM).

Other experiments with a 2-electrode point voltage clamp showed little effect of stretch on the strength-duration curve for threshold contractions. These results suggest a minimal dependence of both charge movement and mechanical activation on sarcomere length in frog skeletal muscle.

Muscle	Sarcomere length (μ)	Q_{max} (nC/μF)	$\bar{V}$ (mV)	k (mV)
Sartorius	2.5	27.9 ± 0.9 (8)	-23.6 (2)	7.5 (2)
Semitendinosus	2.5	26.0 ± 2.0 (3)		
"	3.0	21.1 ± 0.9 (8)	-25.4 (3)	9.4 (3)
"	3.5	24.4 ± 0.6 (3)		
"	3.8	>20		

T-PM-D9 EFFECT OF PROLONGED DEPOLARIZATION ON CHARGE MOVEMENT IN SKELETAL MUSCLE FIBERS.
R.F. Rakowski, Dept. of Physiology and Biophysics, Washington Univ. School of Medicine, St. Louis, MO 63110

Both nonlinear charge and linear capacity decrease during depolarization of frog skeletal muscle fibers in a solution containing 5 mM RbCl, 118 mM tetraethylammonium Cl, 1.8 mM $CaCl_2$, 0.1 μM tetrodotoxin, 467 mM sucrose, 1.5 mM Na phosphate buffer, pH 7.1, 5°C. The time constant of the decrease in linear capacity (T_C) was greater than the time constant of charge immobilization (T_Q). At -40 mV, T_C = 12.8 sec and T_Q = 4.4 sec. At +20 mV, T_C = 0.86 sec and T_Q = 0.28 sec. Charge transient areas (Q) in a fiber held at -80 mV were fit to the equation $Q = Qmax/(1+\exp((V'-Vm)/k)))$, where V_m is membrane potential and V', k and Q_{max} are free parameters. The best fit values were V' = -25.7 mV, k = 12.3 mV and Q_{max} = 18.8 nC/μF. The voltage dependence of charge immobilization was determined in the same fiber by changing the holding potential (V_h). Charge transient areas were fit to the equation $Q = Q_{max}/(1+\exp((V_h-V')/k)))$. The parameter values for charge immobilization were V' = -25.2 mV, k = 11.4 mV and Q_{max} = 18.0 nC/μF. In another fiber the voltage dependence of charge movement was determined at V_h = -80 mV and -45 mV. The parameter values at V_h = -80 mV were V' = -31.7 mV, k = 11.3 mV and Q_{max} = 24.4 nC/μF. The parameter values at V_h = -45 mV were V' = -39.0 mV, k = 11.1 mV and Q_{max} = 13.8 nC/μF. If the rate constant for charge movement (K) is fit to the equation $K = (A(V_m-V')/k) \coth ((V_m-V')/2k)$ the parameter A is 0.036 $msec^{-1}$ for charge transients at V_h = -45 mV and 0.035 $msec^{-1}$ for V_h = -80 mV. These data suggest that charged groups that are moved by a depolarizing step each independently become immobilized during maintained depolarization.

T-PM-D10 MEMBRANE CHARGE MOVEMENT AT CONTRACTION THRESHOLDS IN SKELETAL MUSCLE. M.F. Schneider and P. Horowicz, Dept. of Physiology, University of Rochester School of Medicine and Dentistry, Rochester, N.Y. 14642.

Single skeletal muscle fibers were mounted across a vaseline gap at 2.3-2.6 μm per sarcomere with a 500-700 μm tendon-terminated segment on one side and a cut end on the other side of the gap. The terminated segments were voltage-clamped at a holding potential of -100 mV using the single gap with compensating circuit to monitor both current and voltage, even during contraction (J. Physiol. 277, 483, 1978). Currents I_Q due to intra-membrane charge movement Q were measured when the segment was clamped to a new voltage. In control experiments with contraction blocked the I_Q monitored by the compensating circuit agreed with the I_Q simultaneously monitored by the ΔV between two internal microelectrodes (J. Physiol. 208, 607, 1970). Threshold pulse durations t_{th} for producing just-detectable movement under compound microscope (400 X) with water-immersion objective were also determined for each depolarizing pulse used for monitoring Q. For single step depolarizations t_{th} decreased from 33 to 8 ms as the voltage during the pulse increased for about -45 to about 0 mV, whereas the charge Q_{th} moved during t_{th} was essentially constant over this voltage range. For two-step depolarizing pulses (Fig) in which a 50 ms prepulse to a voltage V_1 below rheobase for movement was followed by a second step to V_2, the total charge $Q_1 + Q_{2th}$ moved at threshold (shaded area) was identical to Q_{th} for a pulse directly to V_2 without any prepulse. This was observed for $Q_1/(Q_1 + Q_{2th})$ of from 0.3 to 0.7. These results indicate that contraction threshold is attained when a set quantity of charge has moved, independent of the manner in which it was moved.

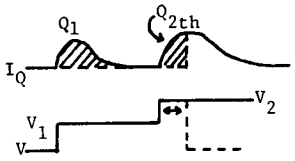

T-PM-D11 CALCIUM TRANSIENTS AND MEMBRANE CHARGE MOVEMENT IN SKELETAL MUSCLE. E. Ríos*, L. Kovács* and M.F. Schneider, Dept. of Physiology, Univ. of Rochester School of Medicine and Dentistry, Rochester, N.Y. 14642.

Light absorbance changes ΔA proportional to changes in free myoplasmic [Ca] and membrane charge movement currents I_Q were monitored simultaneously in isolated frog skeletal muscle fibers with both ends cut and exposed to a 1 mM antipyralazo III-containing solution in a double vaseline gap chamber. The fibers were highly stretched so that ΔA at wavelength λ = 720 nm gave the Ca signal and only at most a small late movement artifact which was subtracted using ΔA at λ = 790 nm. During 100 ms depolarizing voltage-clamp pulses there was a latent period after which [Ca] increased to a peak and then declined toward a steady level. After an initial transition time s_{ON} longer than the latent period the [Ca] time course was consistent with Ca redistribution between three compartments with time-independent rate coefficients. s_{ON} decreased with increasing depolarization ranging from 20-29 ms at -30 mV to 11-18 ms at 0 mV in 4 fibers. It corresponded to the time for membrane charge movement to be about 98% complete. The time s_{ON} required for the rate coefficients for [Ca] redistribution to reach their steady levels may thus be due to the time needed for I_Q to be completed. On repolarization and after a transition time s_{OFF}, [Ca] decayed exponentially to its initial level with a decay time constant which increased as the size of the preceeding depolarization was increased. s_{OFF} was 2-5 ms and was independent of the pulse voltage. It corresponded to the time required for 16-86% of the charge to move back. Ca release thus appears to be turned off before all charge has returned to its resting position. This would be the case if several charged particles participated in the elementary activation event.

T-PM-D12 TUBULAR MEMBRANE POTENTIALS MONITORED BY A FLUORESCENT DYE IN CUT SINGLE MUSCLE FIBERS. J. Vergara and F. Bezanilla, Dept. Physiol., UCLA Med. Sch., Los Angeles, CA 90024.

Single muscle fibers stained with the non-penetrating potentiometric dye WW-781 were voltage or current clamped using the vaseline gap technique modified for optical studies (Vergara and Bezanilla, (1977), Biophys. J. 17:5a). Fibers were illuminated with an exciting wavelength of 625 nm and fluorescence was collected at 180° through a cut-on filter of 665 nm. The ends of the fibers were cut in solutions containing either 120 mM K Aspartate or 60 mM CsF + 60 mM CsAsp as the main ions. External solutions were Ringer's and Ringer's plus 10^{-9} to 10^{-6} M TTX. The fluorescence signals recorded under current clamp conditions showed a slower rising phase and were more spread in time than the membrane action potentials. In fibers perfused with Ringer's solution and under voltage clamp conditions, the fluorescence signals recorded during small depolarizing pulses and any size of hyperpolarizing pulses showed a monotonic rising phase towards a steady level. The time course of the fluorescence signals during large depolarizations was faster and showed a peak that occurred simultaneously with the appearance of a secondary inward current (notch). The "notches" in the current and the peaks in the fluorescence signals were abolished when large concentrations (10^{-7} - 10^{-6} M) of TTX were added to Ringer's. Also, the asymmetry between hyper- and depolarizing pulses was greatly diminished by the use of TTX. Low concentrations of TTX (10^{-9} - 10^{-8} M) were able to partially block the surface sodium current but were less effective in blocking the "notch" of the current and the peak of the fluorescence. Our results suggest that (1) these fluorescence signals arise mostly from the T-system membrane and (2) there is a significant sodium conductance in the T-tubules responsible for the escape of control when the surface membrane potential is voltage clamped.

Supported by MDA and USPHS Grant No. RRO-5354.

T-PM-D13 VOLTAGE OSCILLATIONS AND THRESHOLD PHENOMENA IN CURRENT-CLAMPED BARNACLE MUSCLE. C.E. Morris and H. Lecar, Lab. of Biophysics, NINCDS, NIH, Bethesda, Md. 20014

The ionic conductance system in barnacle muscle is relatively simple - Ca and K conductances which are activated by depolarization and which show no short-time inactivation. The fibers do, however, display a bewildering variety of excitations under constant current stimulation. For example K^+-blocked fibers show bistable plateau action potentials which may persist for several seconds after the current stimulus ceases. When both gCa and gK are operative, complex oscillatory action potentials are elicited over discrete intervals of current. We investigated theoretically the type of behavior that can be expected from two opposing non-inactivating conductances, and showed that a system of three differential equations gives a good account of the threshold, plateau and oscillatory behavior observed in current clamp. Since these phenomena are particularly sensitive to choices of conductance parameters, the model allows us to obtain from current-clamp experiments estimates of these parameters in a way that is largely independent of voltage clamp experiments. A phase-plane analysis of a reduced system of equations, in which the faster of the voltage-dependent conductances is taken to respond instantaneously, is used to explain and predict most of the behavior of barnacle fibers. Substituting a simple non-linear (electrodiffusion) model for the instantaneous gCa produced a more satisfactory facsimile of the plateau potentials than a linear I-V relation. The addition of a slow process, such as Ca accumulation in an internal space, allows us to predict the way in which the slow decline in post-stimulus plateau potentials culminates in a precipitous return to the resting voltage.

T-PM-D14 DEMARCATION POTENTIALS IN MUSCLE PRODUCED BY PROLONGED CURRENT FLOW. Yount, R. A. and Ochs, S. Medical Biophysics Program and Department of Physiology, Indiana University School of Medicine, Indianapolis, IN 46223.

Demarcation potentials in muscle result when the fibers are injured. A similar spread of potential is seen when fibers are subjected to a prolonged depolarization. We have confirmed and extended previous studies (Yount and Ochs, Biophys. J. 21: 167a, 1978) showing demarcation potentials produced by injury to have a length constant of 6.4 mm and the same fibers a length constant of 1.8 mm determined with brief (100 msec) pulses. The larger length constant is not accounted for by conventional cable theory. The injury induced demarcation potentials require 5 to 10 minutes to reach stable values which are then maintained for at least 3 hours. When Cl^- or Na^+ were replaced in the bath with impermeant ions, no effect was found. Thus, this slow change is not due to changes in the ionic permeability ratios of Goldman, Hodgkin and Katz. Our earlier studies showed that it is not due to leakage of K^+ from the injured part of the fiber. An increase in membrane resistance, R_m, could explain the larger length constant, but the R_m measured was actually smaller after injury; a value of 1300 Ωcm^2 was found compared to 4600 Ωcm^2. The time constant of this slow potential change suggests that ion fluxes may be causing local surface concentration changes. To test this supposition, we employed a modified sucrose gap technique which showed that the spread of the injury induced demarcation potential was completely blocked by nonconductive solutions. Furthermore, potential spreads indistinguishable from those induced by injury were produced reversibly by imposing prolonged current flow with an external electrode. We conclude that it is prolonged current flow which causes the spread of demarcation potentials to distances exceeding those expected from conventional cable analysis. Supported by the Muscular Dystrophy Association, Inc.

T-PM-E1 FORMATION AND CHARACTERIZATION OF A REACTION CENTER-LIPID COMPLEX IN AN ORGANIC SOLVENT.† M. Schönfeld, M. Montal, and G. Feher, U.C.S.D., La Jolla, CA 92093.

A complex between soybean phospholipids and reaction centers (RCs) from Rhodopseudomonas sphaeroides R-26 was formed in an organic solvent (hexane) in order to serve as a starting point for incorporating RCs into planar lipid bilayers. The procedure follows that developed for rhodopsin by Darszon, et al.[1] The size of the RC-lipid complex was determined by millipore filtration to be between 150 Å and 500 Å. The optical spectrum of the RC-lipid complex in hexane closely resembles that of purified RCs in aqueous solutions (see Figure). The hexane extract, when supplemented with an excess of ubiquinone-50, exhibited light-induced optical and EPR changes which are typical of RCs. The low temperature kinetics of the (dark) back reaction was found to be the same ($\tau_{(1/e)}$ = 30 msec) as those for chromatophores and purified RCs. Samples of the extract, dispersed in water after evaporating the hexane, showed full photoactivity with no need for quinone addition. Diaminodurene could reduce photooxidized RCs in hexane and also (in its oxidized form) replace the extracted quinone as an electron acceptor. The RCs are thus seen to retain their characteristics, including photochemical activity, in the organic solvent as well as in the aqueous phase after removal of the solvent.

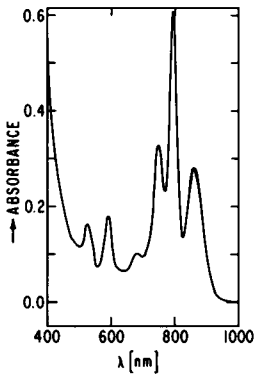

[1]A. Darszon, M. Philipp, J. Zarco, and M. Montal (1978) J. Membr. Biol. 43, 71.

†Work supported by grants from the NSF and the NIH.

T-PM-E2 DISTANCE DETERMINATION IN BACTERIAL PHOTOREACTION CENTERS BY ELECTRON SPIN RELAXATION.† M. K. Bowman,* J. R. Norris and C. A. Wraight, Chemistry Division, Argonne National Laboratory, Argonne, IL 60439 and University of Illinois, Urbana, IL 61801.

The electron spin lattice relaxation times (T_1) in the fast spin diffusion limit have been measured as a function of temperature (T) for the cation radical of the bacteriochlorophyll special pair in purified reaction centers with an intact Fe^{+2}-quinone complex (points F) and with the Fe^{+2} removed (points P) as well as for the semiquinone form of the acceptor in Fe^{+2} free reaction centers (points Q). There is a large, consistent difference in T_1 at all measured temperatures between the special pair cation radical in the Fe^{+2} containing and in the Fe^{+2} free samples as measured using electron spin echo detection of recovery following saturation by a step impulse or picket fence. Interpreting the difference in T_1 as arising from pseudosecular interactions between the special pair and high spin Fe^{+2} allows the special pair Fe^{+2} distance, r_{sp-Fe}, to be calculated. Estimating T_1^{-1} of Fe^{+2} as 6 x 10^9 s^{-1} at 10 K, r_{sp-Fe} is about 24 Å.

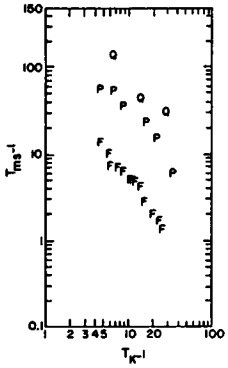

†Work performed under the auspices of the Division of Basic Energy Sciences of the Department of Energy.

T-PM-E3 IN VITRO DUPLICATION OF THE PRIMARY ELECTRON TRANSFER EVENT OF PHOTOSYNTHESIS.† M. J. Pellin,* K. J. Kaufmann* and M. R. Wasielewski, University of Illinois, Urbana, Illinois 61801 and Chemistry Division, Argonne National Laboratory, Argonne, IL 60439.

In reaction centers from R. sphaeroides the dimeric BChl a primary photochemical electron donor absorbs light at 865 nm yielding an excited state which rapidly transfers an electron to a molecule of BPh a in <10 ps. In reaction centers for which the quinone electron acceptors have been either extracted or chemically reduced prior to light excitation BPh a^- back transfers an electron to $(BChl\ a)_2^+$ in 10-20 ns. We now report the first in vitro model reaction center that duplicates both the rapid light induced charge transfer and the slow back reaction of the natural organism. Covalently linked dimers of BChl a, Chl a, and PChl a have been prepared which mimic the spectroscopic and redox properties of reaction center chlorophylls. Treating solutions of these covalent dimers in dry non-nucleophilic solvents, e.g. toluene with molar excesses of a hydrogen bonding nucleophile e.g. primary alcohols results in their folding into a stacked C_2 symmetric conformation. In order to position a pheophytin electron acceptor close to the dimer we have utilized a primary alcohol derivative of pheophytin to induce folding of the dimer into the stacked conformation. In this model the dimer fluorescence is strongly quenched. An excited state difference spectrum obtained immediately following a 6 ps flash at 530 nm (rise time for Δ OD changes <6 ps) may be ascribed to a superposition of dimer cation radical and pheophytin anion radical spectra. Moreover, the spectral changes persist for 10-20 ns with the subsequent return of the ground state absorption spectrum. Thus, we have successfully modelled the fundamental asymmetric charge transfer chemistry of photosynthesis.

†Work performed under the auspices of the Division of Basic Energy Sciences of the Department of Energy and with the support of the National Science Foundation.

T-PM-E4 PHOTOAFFINITY LABELING OF THE QUINONE BINDING SITE IN BACTERIAL REACTION CENTERS OF RPS. SPHAEROIDES.† T. Marinetti, M. Y. Okamura, and G. Feher, U.C.S.D., La Jolla, CA 92093.

2-azido-(^{3}H)-anthraquinone (AzAQ) was prepared and used as a photoaffinity label for the primary quinone binding site in reaction centers from Rhodopseudomonas sphaeroides, R-26. When photolyzed in an organic glass at 80°K, AzAQ gives optical and EPR spectra similar to those expected for a triplet nitrene. When added to reaction centers whose ubiquinone had been removed, AzAQ restored photochemical activity (light-induced bleaching at 865 nm and EPR signals) at 300, 80 and 2.1°K. Hence, AzAQ generates reactive intermediates upon photolysis and replaces ubiquinone as the primary acceptor. Reaction center samples were subjected to strong illumination at 80°K, warmed to allow the nitrenes to couple to the protein and analyzed using SDS gels. The data show selective labeling of the M subunit (see Figure). Control preparations with the quinone site filled by ubiquinone before incubation with the label showed no such preferential labeling of M. These results show that the primary quinone binding site is located at or near the M subunit of the reaction center.

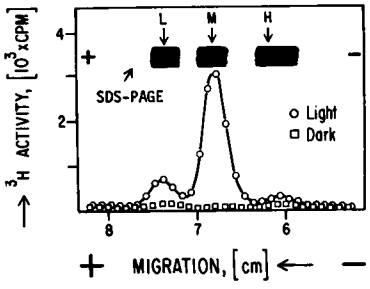

†Work supported by grants from the NSF and the NIH.

T-PM-E5 BINDING OF CYTOCHROME-C TO ISOLATED REACTION CENTERS: ANALYSES BY KINETICS AND EQUILIBRIUM DIALYSIS.† D. Rosen, M. Y. Okamura, and G. Feher, U.C.S.D., La Jolla, CA 92093.

The secondary donor in bacterial photosynthesis is a c-type cytochrome. We have studied the cytochrome binding by kinetic analysis and equilibrium dialysis. Upon laser excitation of RCs in the presence of cyt c, one observes a rapid bleaching (oxidation) of P_{865} followed by a reduction of P_{865}^+ by cyt c. The reduction of P_{865}^+ exhibited biphasic kinetics that were interpreted by the scheme shown in the insert. RCs bound to cyt c exhibit fast kinetics independent of cyt c concentration, while RCs not bound to cyt c give rise to the slow phase (bimolecular collision; dependent on cyt c concentration). While the relative amount of the fast phase is dependent on cyt c concentration, the rate is independent, in agreement with the work of B. Ke, T. H. Chaney, and D. W. Reed [BBA 216 (1970) 373]. Thus, by decomposing the biphasic kinetics we obtained the fraction of the bound species and determined the dissociation constant K_d. For RCs of Rps. sphaeroides in 10mM Tris-Cl, pH 8.0, 0.025% LDAO, T=21°C, the constants are K_d = 0.3μM, $\tau_{1/2}$(fast) ≈ 15μs for horse heart cyt c and K_d = 3.0μM, $\tau_{1/2}$ < 5μs for cyt c_2 (Rps. sphaeroides).[2] At higher ionic strengths (> 0.15M) the fast phase is no longer observed. The kinetics of the slow phase varied with ionic strength in accord with Debye-Hückel theory. Equilibrium dialysis performed at 4°C in 10mM Tris-Cl, pH 8, 0.1% Triton X-100 and varying concentrations (< 50μM) of horse heart cyt c demonstrated 1.1 ± 0.2 cyt c bound/RC and a K_d = 0.5μM, in agreement with the kinetic measurements.

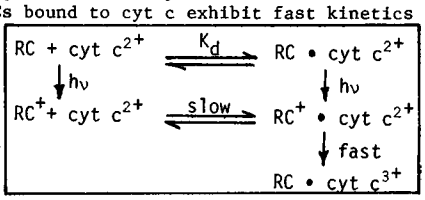

†Work supported by grants from the NSF and the NIH.

T-PM-E6 CROSSLINKING OF CYTOCHROME-C TO ISOLATED REACTION CENTERS.† D. Rosen, M. Y. Okamura, and G. Feher, U.C.S.D., La Jolla, CA 92093.

In the previous abstract we showed that one cytochrome c binds to RCs. In order to localize the binding site we crosslinked cyt c (horse heart) with RCs isolated from Rps. sphaeroides R-26. We used the bifunctional, cleavable reagent, DTBP (dithiobispropionimidate) [Wang & Richards (1974) J. Biol. Chem. 249:8005], and analyzed the products by SDS-PAGE (see Figure). The following results were obtained: RCs incubated with DTBP in 10mM HEPES, pH 8.0 + 0.025% LDAO showed, in addition to the three known subunits (L, M, and H), a strong band with an apparent MW of 44,000 (band Z). When incubated as above in the presence of cyt c two new bands (X and Y), with apparent MWs of 33,000 and 35,000, appeared. They absorbed at 410 nm, indicating that they contained cyt c. From a quantitative analysis of the SDS-PAGE scans, the mole fraction of crosslinked cyt c-RC was 0.3. Using two-dimensional SDS-PAGE (2nd dimension after cleaving with DTBP), we identified Z = L+H; X = L+cyt c; Y = M+cyt c. The crosslinked product, RC-DTBP-cyt c, was isolated by affinity chromatography on a cyt c-Sepharose column which binds RCs but not the RC-DTBP-cyt c complex. The complex showed fast cytochrome oxidation kinetics, even for conditions under which the uncrosslinked species exhibited slow kinetics (e.g., at high ionic strength; see previous abstract). Other crosslinkers, dimethylsuberimidate, dimethyladipimidate, and two azido cyt c derivatives, gave similar crosslinking patterns. These studies show that RCs have a specific binding site for cyt c, which (within the resolution of the crosslinkers) is close to both the L and M subunits.

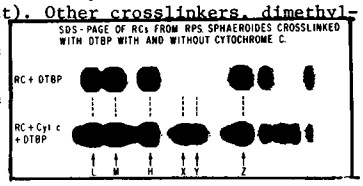

†Work supported by grants from the NSF and the NIH.

T-PM-E7 ORIENTATION OF THE PRIMARY DONOR IN BACTERIAL PHOTOSYNTHESIS. Harry A. Frank*, Richard Friesner*, John A. Nairn*, G.C. Dismukes and Kenneth Sauer (Intr. by T. Wydrzynski), University of California, Berkeley, California 94720.

The triplet state EPR spectra of magnetically aligned whole cells of Rhodopseudomonas viridis and Rhodopseudomonas palustris display a marked dependence on the orientation of the static EPR field with respect to the alignment field direction. This observation implies that the primary donor species on which the triplets are localized are ordered within the membranes. The theoretical model described in a companion paper (Friesner R., Nairn, J.A. and Sauer, K.) was applied to these systems to enable calculation of the orientation of the magnetic axes of the primary donors with respect to the membranes in which they reside. The observed triplet state spectra are generated by an ensemble of partially ordered magnetic systems and a computer similation of the experimental results. The triplet orientation is shown to be very similar for the two organisms studied.

T-PM-E8 TRIPLET QUANTUM YIELDS AND DECAY KINETICS IN DEUTERATED REACTION CENTERS FROM RHODOSPIRILLUM RUBRUM. Robert E. Blankenship and William W. Parson*, Dept. of Biochemistry University of Washington, Seattle, WA, 98195

Photosynthetic reaction centers were prepared from cells of fully deuterated wild type Rhodospirillum rubrum. (Deuterated cells were a generous gift of Dr. Henry Crespi, Argonne National Lab.) The absorption spectrum of the deuterated (D) reaction centers was nearly identical to that of normal (H) reaction centers. The quantum yield of $P870^+$ formation was the same in D and H samples. The halftime of the back reaction between $P870^+$ and Q^- was 78±3ms for H and 84±2ms for D. After reduction of Q with dithionite, the radical pair $P870^+ I^-$ had a decay halftime of 25ns in both samples. At room temperature, about 30% of the decay of $P870^+ I^-$ proceeded via the triplet state of the reaction center carotenoid in both samples. The carotenoid triplet decay halftime was 3μs in H and 6μs in D samples. The identical triplet quantum yields in H and D samples does not support the generally accepted idea that hyperfine interactions are responsible for spin rephasing in the $P870^+ I^-$ radical pair. The smaller magnetic moment of deuterium would give a substantially lower triplet yield unless spin rephasing is always fast relative to the decay of the radical pair. Exchange coupling with reaction center iron also appears not to be important, since iron removal does not decrease triplet yield. Apparently some undetermined mechanism must drive the spin rephasing. In agreement with this conclusion, in H reaction centers from Rhodopseudomonas sphaeroides R-26, the decay of $P870^+ I^-$ into the triplet state begins with no detectable lag, even at low temperatures and in the prescence of magnetic fields. The decay rate at 80°K is slowed from 15ns to 25ns by an 800 G magnetic field.

T-PM-E9 A SECOND MECHANISM FOR SODIUM EXTRUSION IN HALOBACTERIUM HALOBIUM: A LIGHT ACTIVATED SODIUM PUMP. R.E. MacDonald*, J.K. Lanyi, R.V. Greene*, and E.V. Lindley*, (Intr. by R.M. Spanswick), Section of Biochemistry, Molecular and Cell Biology, Cornell University, Ithaca, N.Y. 14853, and NASA-Ames Research Center, Moffett Field, CA 94035.

Whole cells and membrane vesicles prepared from a mutant of H. halobium R_1 accumulate protons in response to illumination (Masuno-Yagi, A., & Y. Mukohata, (1977) B.B.R.C. 78, 237) resulting in a net acidification of the inside of the cells or membrane vesicles. A membrane potential, $\Delta\Psi$, of about - 50 mV is generated by illumination indicating that the net cation flux must be from the inside to the outside of the cells or vesicles. Proton influx takes place only in the presence of Na^+ and is insensitive to the addition of ionophores such as CCCP or 1799, which abolish $TPMP^+$ uptake. Sodium efflux also is stimulated by light in these membrane vesicles and is unaffected by ionophores which abolish membrane potential. Quantitative measurements of $\Delta\Psi$ and $\Delta\mu_{H^+}$ in the presence of these ionophores indicate that $\Delta\bar{\mu}_{H^+}$ is zero or positive (inside). Thus, protons move passively and sodium efflux cannot be driven by an electrochemical gradient of protons. We propose instead that sodium efflux may be driven directly by a light-activated sodium pump similar to, but distinct from bacteriorhodopsin. Proton uptake occurs as a direct result of sodium extrusion by this pump but does not appear to be directly coupled to it.

(supported by NIH Grant GM 23225A; NSF Grant PCM 7609718; NASA Grant NSG 7235)

T-PM-E10 TRANSIENT PROTON INFLOWS DURING FIRST AND SECOND ILLUMINATIONS OF HALOBACTERIUM HALOBIUM. S. L. Helgerson and Walther Stoeckenius, Cardiovascular Research Institute, University of California, San Francisco CA 94143

When freshly harvested H. halobium cells are illuminated under anaerobic conditions the extracellular pH changes show a transient inflow of protons followed by a net acidification of the medium. Our work has centered on separating and defining the contributions of ATP synthesis and ion movements via the Na^+/H^+ antiporter to the observed proton inflows. H. halobium R$_1$A cells can be stored at 4^0 C in the dark for up to 21 days with little or no lysis. During the first illumination after storage, the initial inflow of protons remains unchanged while a second inflow appears at later times. The duration and net alkalinization of this second inflow increase with the length of storage. The duration and net alkalization associated with the second inflow also increase at lower illumination intensity and higher external pH, respectively. Upon second and subsequent illuminations, the first inflow remains unchanged while the second inflow disappears. Experiments correlating the extracellular pH changes with ATP synthesis indicate that the cellular content of ATP reaches a maximum level during the first inflow of protons. This is evident for both the first and second illuminations. Changes in light scattering at an angle of $4^0 \pm 0.5^0$ and a wavelength of 700 nm were followed simultaneously with extracellular pH changes. During the first illumination of cells that have been stored for six days there is an ~20% increase in the intensity of scattered light; no light scattering changes are observed on subsequent illuminations. We interpret these results to show that the first inflow is largely due to the net consumption of protons through ATP synthesis. The second inflow reflects the operation of the Na^+/H^+ antiporter that acts to reestablish the large cation gradients which have relaxed during storage. (NSF PCM-76-11801)

T-PM-E11 ABSTRACT TRANSFERRED

T-PM-E12 ABSTRACT TRANSFERRED

T-PM-E13 THE EFFECT OF CHEMICAL MODIFICATION OF TYROSYL RESIDUES ON PROTON CONDUCTIVITY MEDIATED BY BACTERIORHODOPSIN. P. Scherrer*, C. Carmeli*, P. Shieh and L. Packer, Membrane Bioenergetics Group, University of California, Berkeley, California 94720.

Bleached bacteriorhodopsin mediates protons across proteolipid membranes (FEBS Letters 89, 333-336, 1978). Bleached purple membrane fragments incorporated into liposomes mediate H^+ translocation in response to electrical potentials induced by a K^+ gradient in the presence of valinomycin, and cause collapse of photopotentials formed across lipid impregnated millipore filters generated by bacteriorhodopsin liposomes attached to the planar membrane. These protonophoric activities were inhibited by chemical modification of tyrosyl residues. Thus, iodination of one or more tyrosyl residues blocked proton conductivities mediated by the bleached bacteriorhodopsin, when assayed by either proton fluxes in liposomes or by inhibition of photopotentials formed in lipid impregnated millipore filters. These results indicate involvement of tyrosine both in reprotonation of the retinal Schiff base of bacteriorhodopsin (FEBS Letters 92, 1-4, 1978) and in the movement of the proton through the bleached protein.

(Research supported by the Department of Energy).

T-PM-E14 TEMPERATURE EFFECTS ON THE STRUCTURE AND FUNCTION OF BACTERIORHODOPSIN IN THE PURPLE MEMBRANE. S. -B. Hwang and W. Stoeckenius (Intr. by R. A. Bogomolni), Dept. of Physiology and Cardiovascular Research Institute, Univ. of Calif., San Francisco CA 94143

In the photocycle of bacteriorhodopsin (bR) M_{412} decays more rapidly as the temperature increases. The Arrhenius plot between 7° and 70°C can be approximated by three straight lines of decreasing slope, which intersect at 31° C and at 50°. A more dramatic change in the M decay occurs between 72° and 85°C, where the half decay time actually increases with increasing temperature. Above 85° the decay again becomes faster, but irreversible bleaching of bacteriorhodopsin sets in near 100°C. For a constant stimulus light the fraction of bR molecules which undergo a photocycle also changes with temperature and exhibits sharp discontinuities at the same 30°, 50° and 70°C. The break at 50° shown above may be induced by the change of phospholipid fluidity (lipid-protein interaction) because a sharp X-ray reflection, attributed to the lipid, broadened significantly between 40° and 60°C. The molecular event on the break at 30° is not yet known. The range between 72° and 85°C is the range where Jackson and Sturtevant observed a reversible phase transition where they attributed to a dissociation of the bR lattice in the membrane. Indeed at temperatures above 70°C, we observed change in the X-ray diffraction of the protein lattice (at 80°C only diffused diffraction is detected). And in the flash-induced linear dichroism studies the relaxation constants of 1 msec and 3 msec correlate with a dissociation of the protein lattice. Therefore the break between 72° and 85° is induced by the dissociation of the protein lattice (protein-protein interaction). However, even at temperatures above 85°, the CD splitting in the visible region is still clearly detectable indicating that the bR is not fully dissociated into the monomeric form.

T-PM-F1 DIRECT MEASUREMENTS OF THE STIFFNESS OF ECHINDERM SPERM FLAGELLA. M. Okuno* (Intr. by C. J. Brokaw), Division of Biology, California Institute of Technology, Pasadena, CA 91125.

The echinoderm spermatozoon has a simple "9+2" flagellum. Its stiffness (bending resistance) is the result of the stiffness of the component microtubules and the shear-resistance linkages between the microtubules. Stiffness measurements were made with a flexible glass microneedle (Okuno & Hiramoto, J. Exp. Biol., in press). Stiffness values for several species ranging from 0.3 to 1.5 x 10^{-21} N m^2 were obtained with live spermatozoa immobilized with CO_2. Demembranated sea urchin sperm flagella in an ATP-free solution were about 10 to 20 times stiffer than CO_2-immobilized live ones. The demembranated flagella became more flexible when ATP, without Mg, was added to the solution, but 10 mM ATP was not enough to reduce the stiffness to the level of CO_2-immobilized live spermatozoa. Stiffness values as low as those obtained with CO_2-immobilized spermatozoa were obtained with demembranated flagella in the presence of 1 mM MgATP and .01 mM vanadate, which is a potent non-competitive inhibitor of flagellar movement and dynein ATPase activity (Gibbons et al., (1978) Proc. Nat. Acad. Sci., USA 75, 2220) but does not inhibit relaxation of rigor waves (Gibbons & Gibbons (1978) J. Cell Biol. 79, 285a). These results suggest that MgATP causes detachment of cross-bridges between flagellar microtubules and that vanadate is a reliable reagent for maintaining flagella in a relaxed state by blocking the cross-bridge cycle in a state where cross-bridge attachment is prevented. (Supported in part by NIH grant GM18711 to CJB).

T-PM-F2 REVERSIBLE INHIBITION OF THE FORCE TRANSDUCTION OCCURRING AT THE SURFACE OF FLAGELLAR MEMBRANES. R.A. Bloodgood* (Intr. J. Condeelis). Department of Anatomy, Albert Einstein College of Medicine, Bronx, New York 10461.

Rapid, bidirectional motility of exogenous marker particles occurs in association with the surface of the Chlamydomonas flagellum (J. Cell Biol. 75:983-989, 1977). The velocity of marker movement (2 μm/sec) is load independent and invariable. Flagellar surface motility has been quantitated by measuring the % of attached markers in motion at each time of observation (60% for control populations). The surface motility is reversibly inhibited by 5°C, by raising the NaCl or KCl conc. in the medium, or by lowering the free calcium conc. of the medium below 10^{-6}M using EGTA-calcium buffers or by addition of chelators such as ATP or citrate. When protein synthesis is inhibited by 10 μg/ml of cycloheximide, the flagellar surface motility gradually declines until it is almost totally inhibited at 5 hrs. This inhibition is totally reversed approx. 90 min. after removal of cycloheximide. The ability of the marker particles (polystyrene microspheres) to attach to the flagellar surface also drastically decreases (75% reduction in 5 hrs) during cycloheximide treatment. The effects of cycloheximide on marker adhesion and on the motility of attached markers is greatly reduced if the cells are kept at 2°C during the 5 hr treatment. These data are interpreted to suggest that there is a constant turnover of certain components in the stable Chlamydomonas flagellum. In the absence of protein synthesis, one or more components necessary for marker adhesion and marker motility are eventually exhausted from the flagellum. Further, it is hypothesized that this turnover of flagellar components is greatly retarded in the cold and hence the absence of protein synthesis for the same period of time has a much less drastic effect on the flagellar surface motility. Supported by a Sigma Xi Grant-in-aid and NIH Grant GM 25040 to R.A.B.

T-PM-F3 EFFECT OF VANADATE ON GILL CILIA: SWITCHING MECHANISMS IN CILIARY BEAT. Jacobo Wais and Peter Satir, Dept. of Anatomy, Albert Einstein College of Medicine, Bronx, N.Y.

Lateral (L) cilia of freshwater mussels (e.g. Elliptio) beat with metachronal rhythm when perfused with 12.5mM $CaCl_2$. Addition of 10^{-5}M A23187 causes arrest that has now been demonstrated to be the result of a direct action of increasing Ca^{2+} around the L ciliary axoneme (Walter and Satir, J. Cell Biol. 79, 110). The cilia stop in a specific position, the "hands up" position, i.e. pointing frontally. Recently, vanadate has been shown to inhibit ciliary dynein ATPase (Gibbons et al., P.N.A.S. 75, 2220). Perfusion of mussels gills with ca. 20mM sodium orthovanadate (V), causes the L cilia to stop within 5 minutes. These cilia also stop in a specific position, the "hands down" position, corresponding to the end of the effective stroke, i.e. pointing abfrontally. Arrest can be obtained with exfoliated L cells using ca. 0.5mM V and with triton-treated L cells in 5μM V. In the intact gill we have been able to switch the arrested cilia from one position to another without restarting beat. Upon addition of a solution containing 10mM V, 12.5mM $CaCl_2$ and 10^{-5} M A23187 to L cilia arrested briefly with vanadate, L cilia move to and arrest at a new neutral position where they are approximately straight. Removal of the vanadate from this solution causes some of the L cilia to move towards the hands up position. Conversely, upon addition of both inhibitors to L cilia arrested with Ca-ionophore, L cilia move to and arrest at a neutral position and removal of the Ca-ionophore from the solution causes some of the cilia to move towards the hands down position. These observations suggest that there are two different mechanochemical systems within L cilia that control the initiation, maintenance and direction of the stroke, one sensitive to Ca-ionophore and the second to vanadate. Supported by U.S.P.H.S. Grant HL22560.

T-PM-F4 IDENTIFICATION OF THE MAJOR PROTEIN OF 68,000 MOLECULAR WEIGHT IN MICROTUBULE PREPARATIONS AS A 10-NM FILAMENT PROTEIN AND INVESTIGATION OF ITS EFFECTS ON MICROTUBULE ASSEMBLY IN VITRO. M.S. Runge*, H.W. Detrich, III*, and R.C. Williams, Jr., Department of Molecular Biology, Vanderbilt University, Nashville, TN.

The major protein of 68,000 molecular weight (68K protein) present in cycled microtubule preparations from bovine brain can be isolated in a rapidly sedimenting fraction that consists primarily of filaments 10 nm in diameter. This 68K protein remains in the filament fraction after gel filtration, phosphocellulose (PC) chromatography, or salt extraction. Microtubule protein devoid of 10-nm filaments contains ring structures under depolymerizing conditions, and it polymerizes into microtubules with a characteristically low critical concentration, despite removal of the 68K protein. When cycled microtubule protein is subjected to chromatography on PC, the tubulin fraction (PC-tubulin) assembles into microtubules only at concentrations greater than 2 mg/ml, as others have previously observed. The other fraction, eluted from PC at high ionic strength, contains the 68K protein and can be further resolved into two components by centrifugation. The supernatant, which consists mainly of high molecular weight microtubule-associated proteins, stimulates low concentrations of PC-tubulin to assemble. The pellet contains all of the 68K protein, consists essentially of 10-nm filaments, and does not stimulate assembly of PC-tubulin. Boiling of purified filaments, however, releases several proteins, including the 68K protein. These released proteins stimulate assembly of PC-tubulin. The morphology and protein composition of the filaments isolated from microtubule preparations by these techniques are very similar to those of mammalian neurofilaments. These results suggest that the 68K protein, which may correspond to Tubulin Assembly Protein (A.H. Lockwood (1978). Cell 13, 613) is a constituent of neurofilaments. Supported by Grant GM 25638 of the N.I.H.

T-PM-F5 MICROTUBULE PREPARATIONS AND 10-NM FILAMENTS FROM BOVINE BRAIN CONTAIN ACTIVATABLE CYCLIC NUCLEOTIDE PHOSPHODIESTERASE. P. B. Hewgley*, M. S. Runge*, R. C. Williams, Jr., and D. Puett, Departments of Biochemistry and Molecular Biology, Vanderbilt University, Nashville, TN 37232.

Cycled microtubule preparations from bovine brain were found to contain phosphodiesterase activity using guanosine 3':5'-cyclic monophosphate as substrate. The microtubule preparation was fractionated to give 6S tubulin, soluble microtubule associated proteins, and 10-nm filaments. Phosphodiesterase activity was found in all the fractions, but the 10-nm filament fraction contained the majority of activity. Using a combination of differential centrifugation and gel exclusion chromatography, 10-nm filaments were also prepared directly from brain homogenates and phosphodiesterase activity was identified in this preparation as well. The specific phosphodiesterase activity of the 10-nm filament fractions was between 0.5-1 nmoles/mg filament protein/min. In contrast, the specific enzymic activities of 6S tubulin and the soluble microtubule associated proteins were at most 0.05 nmoles/mg protein/min. The phosphodiesterase activity associated with the 10-nm filaments was stable to several salt extractions and to storage at -70°C. Addition of exogenous calcium-dependent regulator protein to the 10-nm filament preparations resulted in a 1.4-fold stimulation of enzymic activity; the stimulated activity was abolished upon subsequent addition of a chelating agent. Evidence was also obtained for the presence of a phosphodiesterase activator in the 10-nm filament fractions. This factor is calcium-sensitive and heat stable; thus, it may be calcium-dependent regulator protein. This is the first evidence of enzymic activity and a putative regulator associated with this important cytoskeletal structure. (Supported by NIH: GM25638, GM07319, AM00055, RR07089 and RR05424.)

T-PM-F6 ON THE POSSIBLE EXISTENCE OF FUNCTIONALLY-DISTINCT ISO-ACTINS IN PHYSARUM. by M.R. Adelman, Department of Anatomy, Duke University Medical Center, Durham, N.C. 27710.

Actin was isolated from plasmodia of Physarum polycephalum by three procedures chosen to select, in principle, functionally-distinct iso-actins. A protocol which optimizes yield, purity, and biological activity was used to prepare functional actin (FA). DNAase-I affinity chromatography was used to isolate the bulk of the actin (BA) in crude, low salt, plasmodial extracts. Affinity chromatography was also used to prepare, from myosin-rich "differential extracts", the small fraction of actin (DA) not solubilized during the isolation of FA or BA. The DNAase-I studies indicated that virtually all of the 45,000 dalton material in plasmodia is actin. Analyses in one- and two- dimensional IEF and SDS gels showed that FA, BA, and DA all contained a single species of actin with the same pI_{app} as that of rat skeletal muscle. These studies demonstrate that actins isolated so as to maximize the chance of selecting different functional subsets of a putative mixture of plasmodial iso-actins are all apparently identical and contain a single iso-actin. Furthermore, the fact that this single iso-actin has the same pI_{app} in FA, BA, and DA has important implications regarding specific models for the in situ regulation of actin assembly and/or deployment. Supported by NIH grant 5-R01-GM20141 to M. R. Adelman.

T-PM-F7 IDENTIFICATION OF A FACTOR WHICH COPURIFIES WITH SKELETAL MUSCLE ACTIN AND INHIBITS INTERACTION BETWEEN ACTIN FILAMENTS IN SOLUTION. S.D. MacLean* and T.D. Pollard, Department of Cell Biology and Anatomy, Johns Hopkins University School of Medicine, Baltimore, Maryland 21205.

Conventional skeletal muscle actin preparations (Spudich and Watt, J. Biol. Chem. 246: 4866, 1971) contain a factor which inhibits the interaction of actin filaments in solution as measured by low shear falling ball viscometry. The factor binds tightly to actin filaments but not to actin monomers. Hence it copurifies with actin during cycles of polymerization and depolymerization but can be separated from actin by gel filtration at low ionic strength. Conventional actin filament preparations have a reduced viscosity of about 1 cp-ml/mg in an Ostwald viscometer and about 60 cp-ml/mg in our low shear viscometer. Actin separated from the factor has a low shear viscosity of about 750 cp-ml/mg. The factor has no effect on actin polymerization as measured by Ostwald viscometry and by sedimentation. However the factor reduces the low shear viscosity of pure actin from 300 cp to about 1 cp. This complete inhibition of actin filament interactions occurs at low ratios of factor to actin. About 9 µg of crude factor will maximally inhibit the interaction of 0.3 mg actin filaments. The factor is inactivated by boiling or trypsin but not by RNAase. Crude preparations of the factor contain a number of unidentified polypeptides. Different acetone powders vary in their content of this factor, accounting for the variability observed in low shear viscosity of different actin preparations. (Support by grants from NIGMS).

T-PM-F8 THE STRUCTURE OF ACTIN-FASCIN FILAMENT BUNDLES. D. DeRosier and R. Censullo,* Brandeis Univ., Waltham, MA 02154 and K. Edds,* Marine Biology Laboratory, Woods Hole, MA 02543.

F-actin bundles, crosslinked by the 58,000 dalton protein, fascin, have been observed to form upon warming of extracts of sea urchin oocytes (R.E. Kane, J. Cell Biol. 66:305-315, 1975). Nearly identical structures have been seen in the filopodia of sea urchin coelomocytes (K.T. Edds, J. Cell Biol. 73:479-491, 1977). The distinctive features of these bundles are the striations parallel to the axis arising from the actin filaments and the transverse bands about every 110 Å corresponding to the fascin crossbridges. The crossbridges are not evenly spaced but follow a distinctive pattern that depends on the helical symmetry of actin. By applying the techniques of optical diffraction and computer image analysis, we have been able to analyze the pattern of crossbridges, determine with precision the symmetry of the actin and to extract a one-dimensional, filtered image of the fascin crossbridge. The actin symmetry was found to have 2.1590±.001 units/turn. The fascin molecule appears in axial projection as a bilobal peak about 60 Å in length. We have also examined a very similar bundle found in the filopodia of sea urchin coelomocytes. The filopodia contain several proteins but the two most prominent are actin and a 58000K protein (K.T. Edds, J. Cell Biol. 79:263a, 1978). Some of the images show periodic cross-striations every 130 Å and an interfilament spacing of 90 Å. The actin filaments were found to contain 2.160±.0028 units/turn. By comparison paracrystals made from purified coelomocyte actin showed an interfilament spacing of only 66 Å but a nearly identical symmetry 2.157±.001 units/turn. Supported by NIH grants GM21189 (D.D.) and GM 23351 (K.E.).

T-PM-F9 PATTERNED REDISTRIBUTION OF MICROFILAMENTS IN THE LAMELLAR MARGINS OF MOTILE TISSUE CELLS. C. Allen (Intr. by R.B. Scheele), Laboratory of Molecular Biology, University of Wisconsin, Madison, Wisconsin 53706.

Tissue cell translocation on a solid substrate is accomplished, in part, by the production and repositioning of thin (0.1-0.2 µ) lamellar expansions of the cell margin. The physical basis for these movements of the cell margin has been examined by comparative light microscopy of living cells with whole-mount electron microscopy of fixed cells. Ultrastructural observations were made on tissue cells grown on Formvar-coated grids, fixed with glutaraldehyde, further processed by critical-point drying, and then photographed at 1Mev in the High Voltage Electron Microscope. This processing and imaging system maintains the 3-dimensional organization of the whole cell, the relationship of the cell to the substrate, and affords a large sample size which facilitates quantitative analysis. Comparative analysis of film records of living cells with the whole-cell micrographs revealed specific patterns of microfilament organization consistently accompanying recognizable stages of lamellar formation and movement. These results will be discussed in terms of a working model for the mechanics of lamellar motility which includes the following major features: 1) lamellar formation results from an outwardly directed force which relocates microfilaments attached to the interior of the cell cortex, 2) contact of the lower surface of expanding lamellar margins with the substrate triggers a reorientation of microfilaments parallel to the direction of lamellar (and cell) movement, and 3) subsequent interactions between microfilament bundles transmits the advance gained by lamellar expansion to the bulk of the cytoplasm. Supported by NIH grant GM-25133-01. This work was performed at the NIH-supported High Voltage Electron Microscope Facility at the University of Wisconsin-Madison.

T-PM-F10 TORSIONAL MOVEMENT IN INDUCED MONOPODIAL AND POLYPODIAL FORMS OF CHAOS CAROLINENSIS. R.D. Bynum* and R.D. Allen, Dartmouth College, Hanover, N.H. 03755.

Chaos carolinensis is the material of choice for biophysical and physiological studies on amoeboid movement, suitable for many types of experimental manipulation. In healthy cultures polypodial forms predominate, although monopodial forms are occasionally found, especially as cultures age. Specimens of Chaos, cultured in Marshall's medium, that have been centrifuged 30 seconds at 8,000 x g over a cushion of 1% purified agar resume pseudopod formation within minutes of transfer to fresh Marshall's medium. Ca. 10% of these cells become at least temporarily monopodial and exhibit typical "fountain streaming" before and after attachment to the substratum. While some single pseudopodia are straight, others become curved in the plane of the slide. A few form helically shaped pseudopodia. Regardless of pseudopodial form, the tails exhibit torsional motions as they shorten. Some cells exhibit two or more advancing pseudopodia, both of which rotate on their axis relative to the body. Although more difficult to visualize in two dimensional images, it can be seen that polypodial amoebae also exhibit torsion as part of their normal amoeboid movement. This new finding is reminiscent of similar torsional motions that have been described in Nitella, foraminifera, slime molds, and small amoebae.

T-PM-F11 THE ROLE OF CONTRACTILITY IN BLOOD PLATELET FUNCTION. R.D. Allen, L.R. Zacharsky*, and S.T. Widirstky*, Departments of Biology and Medicine, Dartmouth College and Medical School, Hanover, N.H. 03755 and the VA Hospital, White River Jct., Vt. 05001.

It has been suggested on the basis of indirect evidence that human blood platelets contract and may function in a manner analogous to muscle. It is now possible to observe directly by sensitive interference microscopy some of the activities of platelets that previously could be inferred only from light-scattering measurements or electron micrographs of thin sections. Time lapse films of platelet transformation show the shape change from discoid to spheroidal form, extension and retraction of cylindrical pseudopodia, attachment to the substratum, reversible spreading and ruffling of the hyalomere, and the release at all stages of transformation of dense granules containing serotonin and other substances. The gathering of organelles in the central region of the granulomere appears to be due not to a sudden contraction, but to the gradual flow of cytoplasm out of the granulomere region into the hyaline pseudopodia and hyalomere. Evidence for this is that the extension and retraction of each individual pseudopodia is an independent event, just as in amoebae, where each pseudopodium has its own motive force and does not respond to overall changes in intracellular hydrostatic pressure. Similarly, the "release reaction" is not a sudden massive secretion of substances, but a series of discrete exocytosis events of morphologically intact particles. Cytoplasmic contraction may accompany pseudopod extension as in amoebae, and very likely occurs during fibrin clot retraction, provided the platelets form attachments within the fibrin network.

T-PM-F12 IDENTIFICATION OF A SARCOPLASMIC RETICULUM-LIKE SYSTEM IN LEUCOCYTES Maryanna Henkart, Armed Forces Radiobiology Research Institute, Bethesda, Md. 20014.

The endoplasmic reticulum (ER) of the squid axon[1] and of brain synaptosomes[2] sequesters Ca. In neurons the ER forms morphologically specialized appositions with the surface membrane, termed subsurface cisterns (SSC), which resemble the appositions between the sarcoplasmic reticulum and surface membrane of muscle.[3] It has, therefore, been suggested that the SSC in neurons may couple surface stimuli to release of Ca from ER. Similar SSC exist in fibroblasts where some evidence indicates that Ca may be released form intracellular stores in response to mechanical, electrical, or chemical stimuli.[4] In macrophages from mouse peritoneal exudate mononuclear phagocytes from normal human peripheral blood, and cells in macrophage-monocyte producing colonies isolated from mouse spleen,[5] SSC are frequently found in association with areas of membrane involved in phagocytosis or pinocytosis. Human Fc-receptor-bearing lymphocytes, upon contact with surfaces coated with antigen-antibody complexes, flatten and begin to move.[6] In these cells, SSC appear about the same time that 60 A filament arrays, oriented microtubules, and motility begin. Preliminary experiments show that in fibroblasts, macrophages, and lymphocytes the ER contains a dense deposit when prepared for microscopy in the presence of oxalate. These results suggest that a sarcoplasmic reticulum-like system exists in at least some leucocytes. The arrangement of SSC over the cell surfaces suggests that they may be involved in control of cell shape and various forms of motility. Ca release from the ER in response to surface stimuli could represent a form of transmembrane signal in a variety of nonmuscle cells. // 1) Henkart et al. Science (in press). 2) McGraw et al. Soc. Neurosci. Abstr. 1978. 3) Henkart et al. J. Cell Biol. 70, 338, 1976. 4) Henkart and Nelson (submitted). 5) MacVittie and Porvaznik, J. Cell Physiol.(in press). 6) Alexander and P.Henkart J. Exp. Med. 143, 329, 1976.

T-PM-F13 POLYMERIZATION OF LYCOPERSICON ACTIN AND THE ASSEMBLY OF THICK FILAMENTS BY LYCOPERSICON MYOSIN. M. Vahey*, S.P. Scordilis. Dept. Biological Sciences, The University at Albany, 1400 Washington Ave., Albany, N.Y. 12222 and Dept. Biological Sciences, Clark Science Center, Smith College, Northampton, Ma. 01063.

Actin extracted in low ionic strength buffers from the parenchymal cells of the fruit of the tomato, Lycopersicon esculentum was tested for its ability to polymerize in 0.1 M KCl, 2 mM $MgCl_2$ at 37°C. The initial extract protein and the ammonium sulfate fraction could be polymerized whether or not 10 mM EDTA was included in the ammonium sulfate used to fractionate. Electron microscopy of the polymerized ammonium sulfate purified protein exhibited 6 nm wide filaments resembling rabbit skeletal F-actin in their ultrastructure. However, if 10 mM EDTA is included during fractionation further purification by gel filtration on Cl-Sepharose 4B yields two protein peaks neither of which is polymerizable. SDS-PAGE of the larger peak indicates the presence of a major high molecular weight band in addition to the 45,000 dalton band. Cl-Sepharose-4B chromatography of protein prepared without 10 mM EDTA yields a single polymerizable protein pool which exhibits a 45,000 dalton major band and a minor high molecular weight band on SDS-PAGE.

Electron microscopic observation reveals that Lycopersicon myosin forms filaments at low ionic strength. Crude cytoplasmic extracts of parenchymal cells in 0.1 mKCl, 5 mM $MgCl_2$, 6 mM sodium phosphate buffer, pH 7.0 contain characteristic bipolar rods. Thick, 13 nm wide filaments, several microns in length are observed if the ammonium sulfate purified myosin is dialyzed to 50 mM KCl, 1 mM $CaCl_2$, 1 mM imidazole, pH 6.5. Aggregates of short 9 nm wide filaments are observed in the same solution but at pH 7.5

T-PM-F14 THE CALCIUM DEPENDENCE OF HUMAN PLATELET AND BOVINE BRAIN MYOSIN LIGHT CHAIN KINASES IS MEDIATED BY THE CALCIUM DEPENDENT REGULATORY PROTEIN (CDR). D.R. Hathaway*, C.B. Klee* and R.S. Adelstein, NHLBI/NCI, National Institutes of Health, Bethesda, Md. 20014

The myosin light chain kinases isolated from bovine brain and from human platelets can phosphorylate 20,000 dalton myosin light chains purified from turkey gizzard smooth muscle. These two non-muscle myosin kinases require the 16,500 dalton calcium binding protein, CDR, for activity and can be partially purified by affinity chromatography on CDR-Sepharose. The platelet myosin light chain kinase has been purified 170-fold and has a specific activity of 3.1 μmoles of phosphate transferred to 20,000 dalton myosin light chain/mg of kinase/min under optimal conditions. The Km value for ATP is 121 μM while that for light chain is 18 μM. Phosvitin, α-casein, histone II-A, histone f_1 and phosphorylase b do not serve as substrates for the platelet myosin kinase. The myosin kinase isolated from bovine brain and purified through CDR-affinity chromatography is associated with cyclic nucleotide dependent protein kinase (s). Complete separation of these two enzyme activities can be achieved by a second affinity chromatography step on CDR-Sepharose followed by sedimentation in a glycerol gradient. The specific activity of the myosin kinase following glycerol gradient sedimentation is approximately 1.4 μmoles of phosphate transferred/mg of kinase/min, representing a 3000-fold purification.

T-PM-G1 A SIMPLE, ACCURATE THEORY OF IONIC SOLUTIONS. Thomas L. Croxton* and D.A. McQuarrie, Departments of Chemistry, Indiana University and the University of California, Davis, CA 95616.

An approximate theory of ionic solutions that is in excellent agreement with thermodynamic data of the alkali halide salts up to 2 molar concentrations is presented. The theory requires only the solution of the Debye-Hückel equation and well-known statistical mechanical properties of hard sphere systems. Previously this theory has been applied only to Monte Carlo data, but here we discuss its application to real experimental data. This work was supported by a grant from the National Institutes of Health, GM20800.

T-PM-G2 SCATCHARD PLOT ANALYSIS: A GENERAL STATISTICAL MECHANICAL MODEL AND LIMITING SLOPE TECHNIQUE. Ajit K. Thakur and David Rodbard*, Biophysical Endocrinology Unit, Endocrinology and Reproduction Research Branch, NICHD, NIH, Bethesda, MD 20014.

A statistical mechanical approach is used to describe binding isotherms, including receptor multivalency, heterogeneity and/or cooperativity. Special cases studied were nearest neighbor and all-possible pairwise interactions. For the Scatchard plot (B/F vs B), the limiting intercepts and slopes for bivalent receptors are:

$$I_o=n_o\langle K\rangle,\ S_o=(b-2)\langle K^2\rangle/\langle K\rangle,\ I_\infty=n_o,\ S_\infty=-b/\langle K^{-1}\rangle;$$

for the "competitive binding inhibition" curve (B/T vs T), the corresponding values are:

$$I_o=n_o\langle K\rangle/(1+n_o\langle K\rangle),\ S_o=(b-2)n_o\langle K^2\rangle/(1+n_o\langle K\rangle)^3,\ I_\infty=\infty,\ S_\infty=0,$$

where b 1 and b 1 correspond to positive and negative cooperativity, respectively, n_o is the Total concentration of receptor sites and $\langle K^i\rangle$ denotes the i^{th} moment of the affinity distribution around the origin. Several numerical methods are available to describe the B/T vs T curves using empirical models (hyperbolic, polynomial, cubic spline functions) appropriate to the particular situation. The results are mapped back into the Scatchard coordinates, and the limiting slopes and intercepts of these plots permit ready calculation of the binding parameters. Depending on experimental design, these may be of adequate precision, or they may be further refined by weighted nonlinear regression with mechanistic models. This approach appears to be a valuable addition to the extensive repertoire of analytical methods for ligand binding systems.

T-PM-G3 COUPLING OF SPONTANEOUSLY BEATING MYOCYTES IN TISSUE CULTURE. S. Scott* (Intr. by R. Spangler), State University of New York at Buffalo, Buffalo, New York 14214

Experiments were performed on spontaneously beating myocyte clumps to elucidate their oscillator characteristics. 100μ diameter clumps were prepared from 9 day old embryonic chick hearts and tissue cultured for 3-4 days before use. Recording was by microelectrode in a balanced bridge circuit so that simultaneous current injection and voltage measurement was possible. Three types of experiments were done: (1) single current pulses were injected in order to construct the phase response curve; (2) free running pulses of various frequencies and intensities were injected to measure the clumps ability to follow pulse trains; (3) synchronization between two isolated clumps was obtained by simulating the nexus junction with the external electronics. Assuming the nexus to be a linear conductance g_n, nexus current, i_n, could be injected into each clump as $i_n = g_n (V_{m1} - V_{m2})$, where $V_{m1} - V_{m2}$ is the measured potential difference between the two clumps. The results of the experiments were then correlated with digital simulations of FitzHugh's BVP excitable cell model in situations analogous to the experimental conditions.

T-PM-G4 PARTITIONING THE RHYTHMIC WAVEFORMS INTO A SET OF STATES. C. M. Winget, Ames Research Center, Moffett Field, CA 94035, N. W. Hetherington,* and L. S. Rosenblatt,* Geneticon, 748 Minert Road, Walnut Creek, CA 94598.

The biologic rhythm waveform is partitioned into a set of 8 "states", each representing a portion of the waveform which has physiological meaning. We estimate for each data point successively a rate of change and relative level with respect to the mean. Four states represent the peak, trough and ascending and descending means. The remaining 4 states represent the ascending and descending transient states. The method is based on estimating successively the slope of 5 contiguous data points, adding and dropping one in turn. We then utilize the estimates of the slopes to divide the rhythm into a set of 8 states and define the rhythm in terms of those states. We define a period as the time required to traverse the 8 states and are able, therefore, to estimate periodicity from even short stretches of data. The absolute and relative times spent in each state may also be estimated. This method has significant application qualities;e.g., the chronopharmacologist (CP) is able to determine differential effectiveness of a drug relative to the rhythm state. It is also possible to determine effectiveness of drugs relative to a set of states derived from several physiological parameters. The power of this method is that it enables the CP to disassociate the waveform from the real-time clock and to operate in the domain of the biological clock. By being able to estimate the rhythm state, the CP can be more precise in judging drug effects. Deviations from the expected circadian rhythmicity such as transient periodicities may be detected and taken into account.

T-PM-G5 THREE-DIMENSIONAL CABLE THEORY: A BI-DOMAIN MODEL. L. Tung*(Intr. by M. Morad), Massachusetts Institute of Technology, Cambridge, MA 02139.

A "bi-domain" model has been formulated to describe macroscopic potentials in electrically coupled cellular tissues. The intracellular and extracellular volumes form two domains which overlap at every point in space but are separated by a volume-distributed membrane boundary whose electrical properties are represented by a current source in parallel with a resistance. The membrane current source is in turn represented by a pair of coupled, complementary monopole sources in the two domains. Ohm's law and charge conservation are written in each domain to account for the new structure, and the following equations can be derived, subject to the appropriate contraints at the boundaries to the bi-domain system:

$$\nabla^2\Phi_m = (1/\lambda^2)\Phi_m - (P_o+P_i)U_{ms} + P_oU_{os} - P_iU_{is} \quad (1)$$

$$\nabla^2\Phi_o = -(P_o/(P_o+P_i))\nabla^2\Phi_m - P_E(U_{os}+U_{is}) \quad (2)$$

$$\nabla^2\Phi_i = (P_i/(P_o+P_i))\nabla^2\Phi_m - P_E(U_{os}+U_{is}) \quad (3)$$

where Φ_o,Φ_i,Φ_m = extracellular, intracellular, and transmembrane potentials (V); P_o,P_i = macroscopic extracellular and intracellular bulk resistivities (Ω-cm); $P_E = P_oP_i/(P_o+P_i)$ (Ω-cm); λ = space constant (cm); U_{os},U_{is} = externally applied extracellular and intracellular current point sources (amp/cm^3); U_{ms} = "volumetric" membrane current source (amp/cm^3). From the above equations the potentials and current densities in each domain can be separated into "differential-mode" and "common-mode" components, with the former arising from U_{ms} and the latter arising from U_{os}, U_{is}, and boundary effects. The results of this analysis have been applied to describe baseline shifts in the electrocardiogram following acute ischemic injury.

T-PM-G6 ELECTROSTATIC CALCULATIONS FOR AN ION CHANNEL IN CONTACT WITH AN ELECTROLYTE SOLUTION. B.E. Enos and A. Peskoff, Dept. Physiol., UCLA Medical School, Los Angeles, Ca. 90024.

In order to estimate the electric potential seen by an ion inside a channel, the following model is considered. The membrane is represented by a dielectric slab (ε_2=2) containing a cylindrical channel (ε_1=6 to 80). The membrane is immersed in an electrolyte solution (ε_3=80) of ionic strength μ. The calculation includes the effects of induced polarization charge on the cylindrical and planar surfaces, and space charge in the electrolyte. For $\mu=\infty$, an analytic solution is obtained for the potential. This solution is also the Green's function for the potential inside the membrane with Dirichlet boundary conditions on the two planar surfaces and, as such, can be used to calculate the potential inside the membrane from its value on these surfaces. The potential in the half-spaces containing an assumed Debye-Hückel electrolyte satisfies the Helmholtz equation. The Green's function for Neumann boundary conditions is known and can be used to calculate the potential in the electrolyte from its normal derivative on the two planar surfaces. An iteration scheme to calculate the potential for arbitrary μ is set up using these two Green's functions, the appropriate boundary conditions on the planes, and an initial trial surface potential. For a channel with dimensions of gramicidin A, the single-ion potential barrier for this model, for large μ, can be up to 10 kT higher than that calculated by Levitt at μ=0 (Biophys. J. 22:209 (1978)). Electrolyte effects may therefore contribute to the dependence of gramicidin A I-V's on ion concentration (c_i), and, in particular, their hyperbolic shape at large c_i. The calculation also can be done for multiply occupied channels, and indicates that it is energetically possible to have three or more ions in the channel for large c_i. Supported by USPHS (F32 GM05786, NS09931, 5 K04 GM00222) and NSF (PCM 7620605).

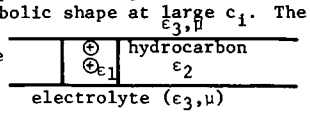

T-PM-G7 IN VITRO CHEMICAL CARCINOGENESIS IN SYRIAN HAMSTER EMBRYO CELLS BY MNNG. P.Rosen, Univ. Massachusetts, Amherst, MA 01003.

The author has calculated transformation frequencies for ultraviolet light in vitro carcinogenesis using mutation frequencies of AGr locus with good results[1]. For the aklyating agent MNNG, Myhr and DiPaolo have measured mutation frequencies in Syrian hamster cells, finding 2.4×10^{-3} mutations per survivor at 10 μM concentration[2]. Also Coulondre and Miller[3] have found that 14% of mutations in the regulator gene of the lac operon are chain terminating. Assuming that mutations in both the operator region and nonsense mutations in the regulator gene of the operon controlling mitosis causes transformation, we have calculated transformation frequencies vs concentration which agree very well with DiPaolo et al[4]. The slope of the measured transformation frequency vs concentration is 2.6×10^{-4} per $\frac{\mu g}{m\ell}$. The calculated value of the slope is 2.7×10^{-4} per $\frac{\mu g}{m\ell}$

[1]P. Rosen (1978), American Soc. Photobiol. June 11-15, Burlington, Vt.
[2]B.C. Myhr and J.A. DiPaolo (1975), Genetics 80, 157.
[3]C. Coulondre and J.H. Miller (1977), J.Mol. Biol. 117, 525.
[4]J.A. DiPaolo, R.L. Nelson and P.J. Donovan (1972), Nature 235, 278.

T-PM-G8 ENERGY LOAN MODEL OF ENZYME CATALYSIS. Michael Conrad, Computer & Comm. Sciences, University of Michigan, Ann Arbor, MI 48109.

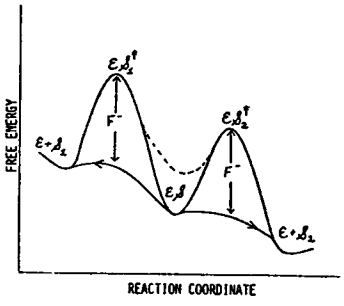

The free energy changes accompanying enzymatic reactions can be re-interpreted in terms of a two-pathway construction (called an energy loan diagram). The lower pathways (with arrowheads) are decomposition pathways which can only be entered from the complexed state, which is unstable. The minimum of the dashed line is the apparent free energy, as determined by kinetic measurements under the assumption that the complex is stable. The real free energy of the unstable complex is described by the solid-lined minimum. The diagram suggests a mechanistic interpretation in which the instability derives from the formation of short-lived electron pairs in the complexed state, with the activation energy advantage (F^-) deriving from the nuclear motion produced by the resulting orbital instability. The pairing interaction can be formally described in terms of a complex-imposed reduction in the difference between the arguments of the spatial eigenfunctions of two electrons, where the properly antisymmetrized complete eigenfunction consists of an antisymmetric spatial and symmetric spin component. The antisymmetric spatial component is replaced by a distinguishing antisymmetric eigenfunction. The interaction can be pictured in terms of a constraint on an internuclear distance which causes two anticorrelated electrons to be repelled from one another less strongly than they are attracted to the positive nuclei.

T-PM-G9 CUSP CATASTROPHE AND HYSTERESIS: AGGRESSIVE-SUBMISSIVE BEHAVIOR OF DOGS. Peter Fong, Emory University, Atlanta, Georgia 30322.

The catastrophe theory of René Thom has been applied to problems in many fields including biology involving discontinuity and divergence.[1] The impression is given that the conventional scientific method (essentially Newtonian) is unable to deal with such problems and the void is filled by the new mathematical theory. Using the bimodal behavior of dogs as an example, it is shown that the phenomenology on the behavior level described by the cusp catastrophe can be analysed by the conventional scientific method and reduced to a hysteresis effect on the physiological level which can be tested by experimental investigation. The use of the catastrophe theory thus not only reveals no new information but also confuses the investigation of the real issue. Phenomenologically the point of change from aggressive to submissive behavior by frightening an enraged dog does not coincide with the point of the reversed change by enraging a frightened dog. The change of the behavior state ranging from retreating, cowering, avoiding, neutrality, growling, snarling, and attack is discontinuous (analogous to domain rotation in magnetism). It appears that an amount of "activation energy" is involved in each change, leading to a hysteresis effect on the behavior (analogous to magnetization). The bimodal behavior can thus be explained. The hysteresis effect can be ascertained by studying experimentally the correlation of the stimulus with the amount of adrenalin in the blood stream and with the behavior state. Thus the behavior can be explained by physiology as we expected it to be according to the conventional scientific method.

1. E. C. Zeeman, Catastrophe Theory, Addison-Wesley, Reading, Mass. 1977.

T-PM-G10 MECHANICS OF THE BIOPHYSICAL STATE - A NEW MECHANICS.
Arthur Gropper, former Biophysics Department, Univ. of California, Los Angeles, California, 90024.

A more definitive geometrical theory of space and time, originally reported six years ago, is presented.[1] A biophysical state is considered as a system in quasi-static equilibrium, whose change follows from a variation of entropy considered as k ln W. The variation principle is conceived as a geometric scheme in a special space-time manifold which in its local properties follows Poincare' geometry in a hyperbolic plane and in its global properties traces out a helical curve.

1. A. Gropper, Biophysical Society Abstracts, 17th Annual Meeting, 38a, (1973).

T-PM-G11 CHAOS IN ENDOCRINOLOGY
R. Rössler and F. Götz (Med. Univ.Poliklinik) and O.E. Rössler* (Institute for Phys. and Theor. Chem.), Univ. of Tübingen, 7400 Tübingen, W. Germany

Most endocrinological homeostatic mechanisms (like the hypothalamus-pituitary-adrenal-cortex loop) involve at least 3 variables. Three-variable control systems are capable of chaotic oscillations, however. Example:

$$\dot{x} = -x + f(z)\ , \qquad \dot{y} = x - y\ , \qquad \dot{z} = y - z\ , \tag{1}$$

with $f(z)$ a smooth $\wedge$-shaped function ($f(z) = -.25 - 9g(z) + \sqrt{100g^2 + 10^{-4}}$) and initial conditions $x(0)=.1$, $y(0)=.3$, $z(0)=.4$, for example. The more intermediate variables and/or delay, the more likely is chaos. Eq.(1), with an $\wedge$-shaped $f(z)$, was first considered as a model of pituitary-thyroid homeostasis by L. Danziger and G.L. Elmergreen in 1956 (Bull. Math. Biophysics 18, 1-13). Similar models apply to blood glucose regulation (compartmental interpretation of Eq. 1), renin homeostasis, etc. In order to test the chaotic hypothesis, short-interval (less than one minute) measurements of 2 variables in the above named loop (plasma cortisol and plasma ACTH) were performed in 2 volunteers over 60 minutes in supine position. The phase plot trajectories will be presented. Preliminary conclusion: The observed rapid irregular oscillation may be due to an autonomous mechanism. If correct, nature would use an oscillatory (and even chaotic) 'mean steady state' as its object of control. Such an organization was predicted by M. Conrad (personal communication 1976). $^*g(z) = 3.6 - 8.4z$

T-PM-G12 SINGLE DOMAIN PARTICLES AND MAGNETOTATIC BACTERIA. Charles P. Bean, General Electric Corporate Research and Development, P.O. Box 8, Schenectady, New York 12301

Blakemore[1] has discovered a class of anerobic bacteria that exhibit a magnetotactic response in the earth's magnetic field. Electron microscope studies coupled with x-ray emission measurements reveal chains of iron-rich particles in the body of the bacteria. Blakemore suggested that the chains might serve as magnetic dipoles to provide an orienting torque in a magnetic field. In a private communication, E.M. Purcell pointed out that the particles might be single magnetic domains. On this hypothesis it is possible to write an equation of motion for the passive orientation of the bacteria as $\dot{\theta} = -M_S B_o V \sin\theta / 8\pi\eta R^3$ where θ is the angle between the field B_o and the moment associated with a magnetization M_S in a saturated ferromagnet of volume V. The bacterium is approximated as a sphere of radius R in a fluid of viscosity η. For reasonable parameters, the volume of Fe_3O_4 required to accomplish rotations in one minute in the earth's field, would amount to only two spheres $\sim$400Å in diameter or four spheres $\sim$300Å in diameter, etc. The observed electron dense regions are significantly larger. The theory[2] of the magnetization of "chains of spheres" of magnetic single domains gives specific values for the coercive force ($\sim$350 Oe for a chain of two spheres of magnetite) and predicts a non-monotonic dependence of coercive force on the angle of the applied field relative to the chain.

[1] R. Blakemore, Science 190, 377 (1975).
[2] I.S. Jacobs and C.P. Bean, Phys. Rev., 100, 1060 (1955).

T-PM-G13 ANTIBACTERIAL EFFECT OF ELECTRICALLY ACTIVATED SILVER AND CERIUM STEARATE IN MONOMOLECULAR LAYERS ON SURGICAL IMPLANTS. G. Colmano, S. S. Edwards,* and T. E. Lesch,*
Dept. Veterinary Science, VPI & SU, Blacksburg, VA 24061

Silver (Ag) and Cerium (Ce) stearate in monomolecular films, deposited on stainless steel intramedullary pins, were activated by one hour of 12 microamperes of positive direct current per cm^2 (12 μAH+DC/cm^2). This treatment proved bacteriocidal for up to 3000 *Staphylococcus aureus* and 500 *Proteus vulgaris* contaminating the pin's surface. Two pins were contaminated by bacteria and were inserted either *in vitro* (petri dishes, agar vials, and broth tubes), or *in vivo* (rabbit and dog femurs). After current application, they were extracted and cultured. Only the pins that were treated with current displayed the bacteriocidal effect; this was attributed to the activation of Ag and Ce ions by 12 μAH+DC with the stearate monomolecular film providing a carbon matrix support that facilitated their activities. The ionic motility in the $Ag^+/AgCl/Cl^-$ electrode distribution of charges was correlated to the bacteriocidal effect to explain the empirical findings. This project was supported by VPI & SU Research Division Supplemental Funds.

T-PM-G14 DIASTOLIC PRESSURE-VOLUME RELATIONS AND DISTRIBUTION OF FIBER EXTENSION IN A MODEL LEFT VENTRICLE.
Theodore S. Feit (Intr. by Mu-ming Poo), Univ. of Calif. Irvine, Irvine, Calif. 92717

A model for left ventricular diastolic mechanics is formulated which takes into account non-negligible wall thickness, incompressibility, finite deformation, non-linear elastic effects, and the known fiber architecture of the ventricular wall. The model consists of a hollow cylindrical mass of muscle bound between two plates of negligible mass. The wall contains fiber elements which follow a helical course and carry only axial tension. To simplify the analysis and reduce the number of degrees of freedom, the anatomic distribution of fiber orientations is divided into a clockwise and counter-clockwise system. An equation representing the global condition for equilibrium is derived and solved numerically. It is found that the model's pressure-volume relation is representative of diastolic filling *in vivo* over a wide range of filling pressures, and the calculated mid-wall sarcomere lengths in the model compare favorably with published experimental data. Subendocardial fibers are stretched beyond L_{max} even at low filling pressures, i.e. 5 mm Hg, while fibers located between 60-80% of wall thickness extend minimally between 5-12 mm Hg. The hydrostatic pressure field within the wall is highly non-linear. The pressure rises steeply in the subendocardial layers so that the net gain in pressure in the inner third of the wall is 85% of the filling pressure. It is demonstrated that these results are independent of heart size for a family of heart models which are scale models of each other. They are, however, critically dependent on the existence of longitudinally oriented fibers in the endocardial and epicardial regions of the heart wall.